X-321-69-474
PREPRINT

DEVELOPMENT OF REALISTIC VIBRATION TEST LEVELS FOR SOUNDING ROCKET SUBSYSTEMS

R. L. KINSLEY

SEPTEMBER 1969

GODDARD SPACE FLIGHT CENTER
GREENBELT, MARYLAND

X-321-69-474

DEVELOPMENT OF REALISTIC VIBRATION TEST LEVELS FOR SOUNDING ROCKET SUBSYSTEMS

R. L. Kinsley
Structural Dynamics Branch
Test and Evaluation Division

September 1969

GODDARD SPACE FLIGHT CENTER
Greenbelt, Maryland

DEVELOPMENT OF REALISTIC VIBRATION TEST LEVELS FOR SOUNDING ROCKET SUBSYSTEMS

Prepared by: Ronnie L. Kinsley

Ronnie L. Kinsley
Structural Dynamics Branch

Reviewed by: Edward J. Kirchman

Edward J. Kirchman
Head, Structural Dynamics Branch

Approved by: John H. Boeckel

John H. Boeckel
Deputy Chief, Test and Evaluation Division

PROJECT STATUS

Personnel of the Structural Dynamics Branch felt that the methods used for testing sounding rocket subsystems could be improved. This report summarizes the results of an investigation which confirms this belief.

AUTHORIZATION

Test and Evaluation Charge No. 321-879-60-25-01

DEVELOPMENT OF REALISTIC VIBRATION TEST LEVELS FOR SOUNDING ROCKET SUBSYSTEMS

Ronnie L. Kinsley

SUMMARY

Sounding rocket subsystems are currently vibration tested to the same exposure levels as the payload, a process which ignores the transmissibility of the payload structure. This is done because specific transmissibility data is not available for each of the hundreds of sounding rockets launched each year. An investigation was undertaken, using the NIKE-APACHE rack as a typical example, to determine whether transmissibilities fall within a predictable range when certain key parameters (weight and c.g. location) are varied. If so, subsystem specifications having predictable tolerances could be developed which would take into account the transmissibility and thus be superior to the current specifications which ignore transmissibility entirely.

Using a combination of analytic and experimental techniques, it is shown that this can be done, and furthermore specific recommendations for modifications of system level specifications are made for the testing of NIKE-APACHE subsystems.

CONTENTS

ILLUSTRATIONS

ILLUSTRATIONS (Continued)

TABLES

DEVELOPMENT OF REALISTIC VIBRATION TEST LEVELS FOR SOUNDING ROCKET SUBSYSTEMS

INTRODUCTION

The specifications for sounding rocket vibration tests have generally been determined by analyzing data taken during test flights. Flight accelerations are measured at the point where the payload interfaces with the rest of the rocket. (In the case of the NIKE APACHE, the payload interfaces with the APACHE motor.) This flight vibration is simulated during a test by mounting the payload on the shaker and inputing the desired vibrations at the payload/shaker interface. Such a test set-up is thus consistent with the flight condition, since the vibrations are controlled at the same point at which flight measurements are taken.

In addition to design qualification and flight acceptance vibration tests at the "systems" level of assembly, it is often desirable to subject individual subsystems to vibration prior to integration with the payload or spacecraft. In the case of major spacecraft projects, the subsystem specifications are usually derived from data acquired during tests of a structural model of the spacecraft. These subsystem specifications take into account the transmissibility of the structure between the driving point interface and the point of attachment of the subsystem.

In the case of sounding rockets, however, this practice has not been followed since there are generally no structural models or prototypes of the payloads. Instead, subsystems are tested to the same specifications as the entire payload, neglecting stuctural amplifications.

While each payload is different, there are similarities among them. In each sounding rocket type, a more or less "standard" rack structure is used, and payload mass properties usually fall within a certain limited range.

The purpose of the study described herein was to determine, by investigating the range of responses induced by a variation in payload configuration, whether a subsystem vibration test specification could be obtained which would more closely approximate the behavior of the subsystems under flight conditions than current practice allows.

ANALYTIC STUDY

Before any testing was performed a brief analytic investigation was made to determine the theoretical resonant frequencies of the structure. In the lateral axis the normal mode method was used to determine the first four resonant frequencies and their associated mode shapes. A computer program provided this information. The only necessary inputs to the program were the flexibility and mass matrices of the system. To obtain these matrices the following mathematical model of the system had to be defined. The payload structure was defined as a series of lumped masses located at specific stations and connected by a massless beam of stiffness K (lb/in). This stiffness was experimentally calculated by a series of static deflection tests. Figures 1 and 2 present pictures of the static deflection test set-up for the rack and the rack/shroud combination respectively. (These test items are described in detail in the next section.) From this information the first four lateral resonant frequencies were computed. The program provided the corresponding mode shapes by normalizing the deflections at each station to the maximum deflection.

In the thrust axis the fundamental frequencies of the longerons and the shelves (see section entitled TEST SET-UP AND INSTRUMENTATION) were calculated. This was done by considering the shelves as semi-simply supported plates. After compensating for the weighted condition the natural frequency of the shelves was determined to be in the neighborhood of 100 Hz, while that of the longerons was determined to be approximately 500 Hz.

All of the analytic calculations for the lateral response of the system were made for two configurations. The first configuration was that of the loaded rack (for five different payload mass distributions), while the second configuration was that of the loaded rack/shroud combination (for the same five different payload mass distributions). The corresponding mode shapes are shown in Figures 3 thru 8. It can be seen that a change in total weight does not affect the mode shape, but that a rearrangement of the weights (i.e., different c.g. location) does affect the mode shapes. Comparing the two conditions shows that the resonant frequencies of the rack/shroud combination are higher than those of the rack alone. This is obviously the case since the shroud adds a great deal of stiffness but relatively little mass.

A brief discussion of the correlation between the theoretical predictions and the experimental results is presented in the last section of this report.

TEST SET-UP AND INSTRUMENTATION

The test item was a NIKE APACHE payload rack, consisting of six shelves bound together by four longerons. Under flight conditions this rack is encased

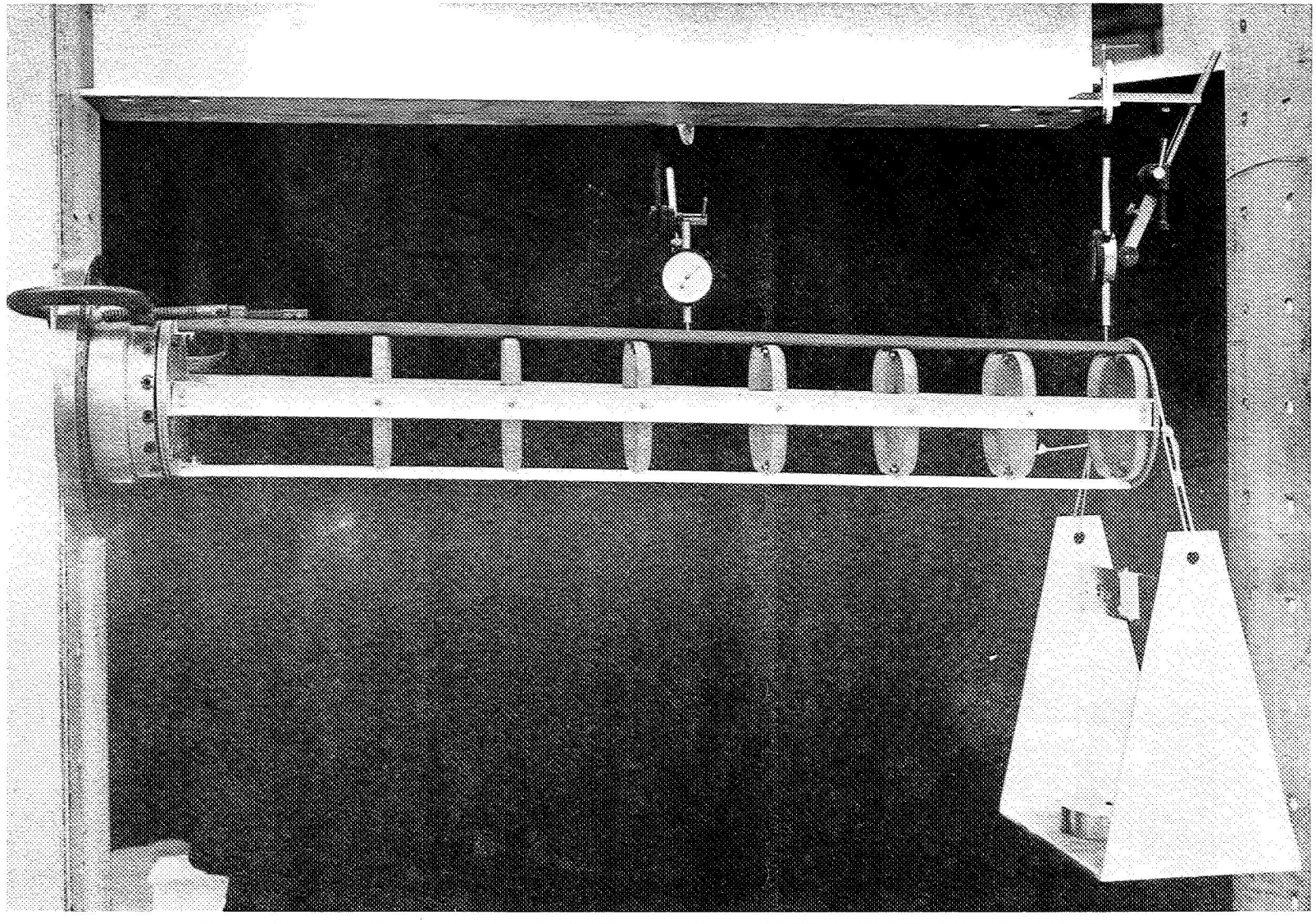

Figure 1. Test Set-up for Static Deflection Test of NIKE-APACHE Payload Rack

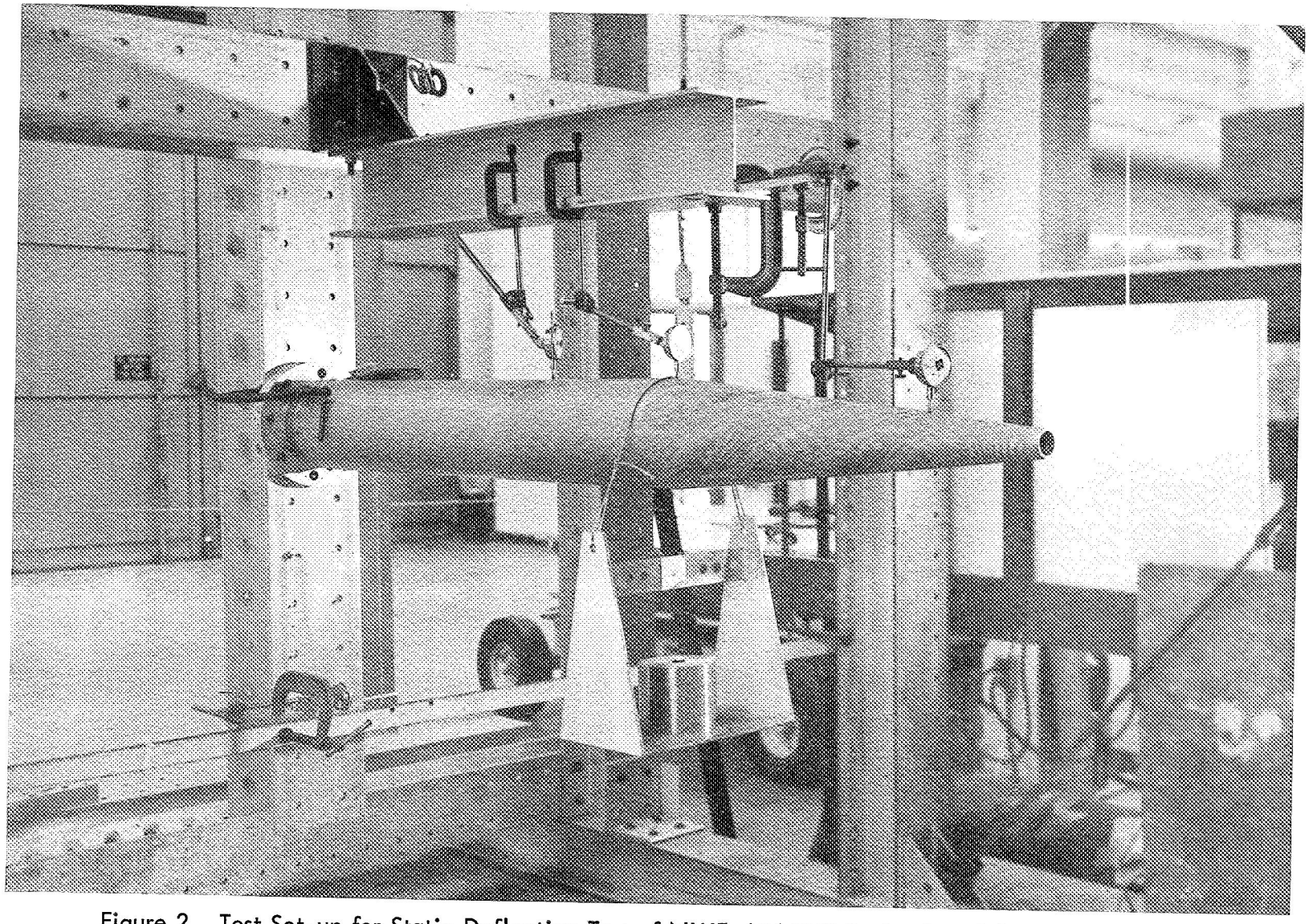

Figure 2. Test Set-up for Static Deflection Test of NIKE-APACHE Payload Rack/Shroud Combination

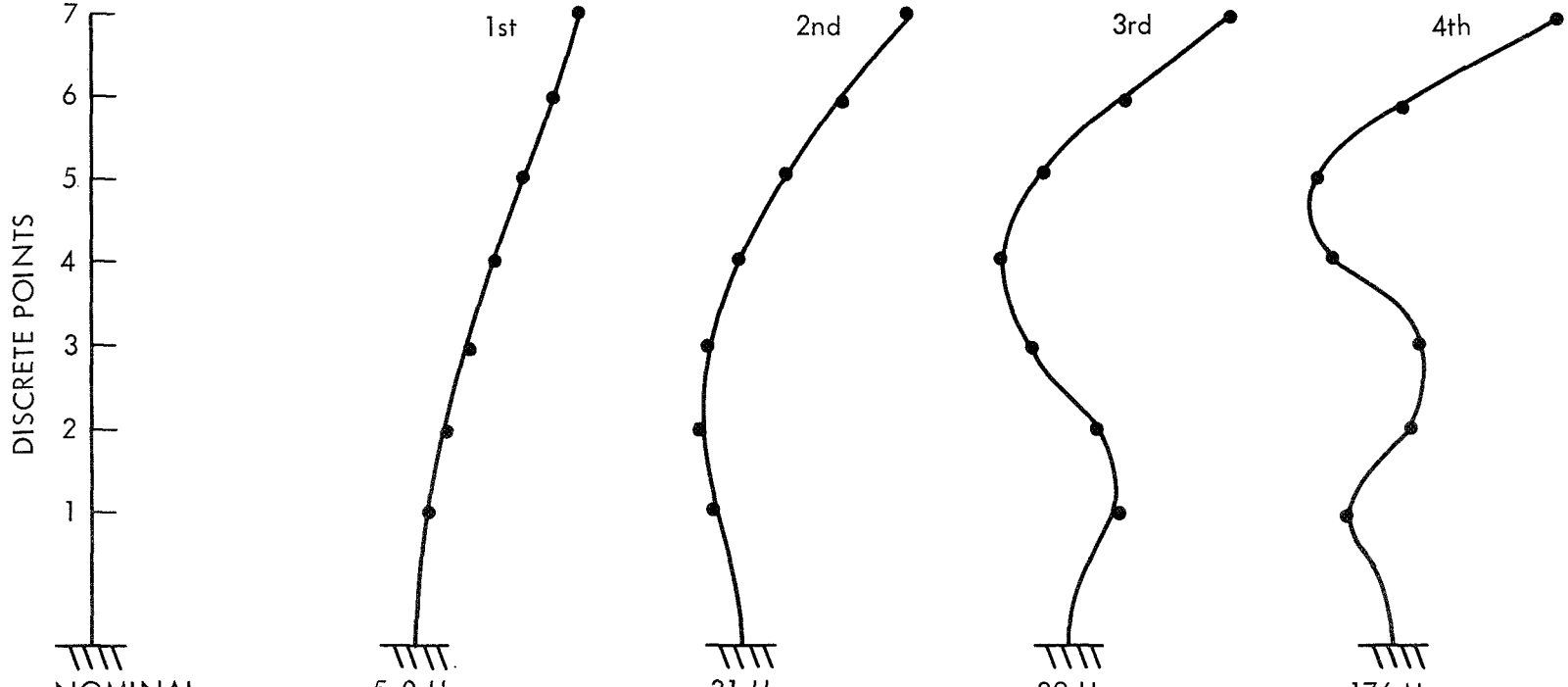

Figure 3. Rack only—Three Uniformly Distributed Payloads (Nominal C.G.)

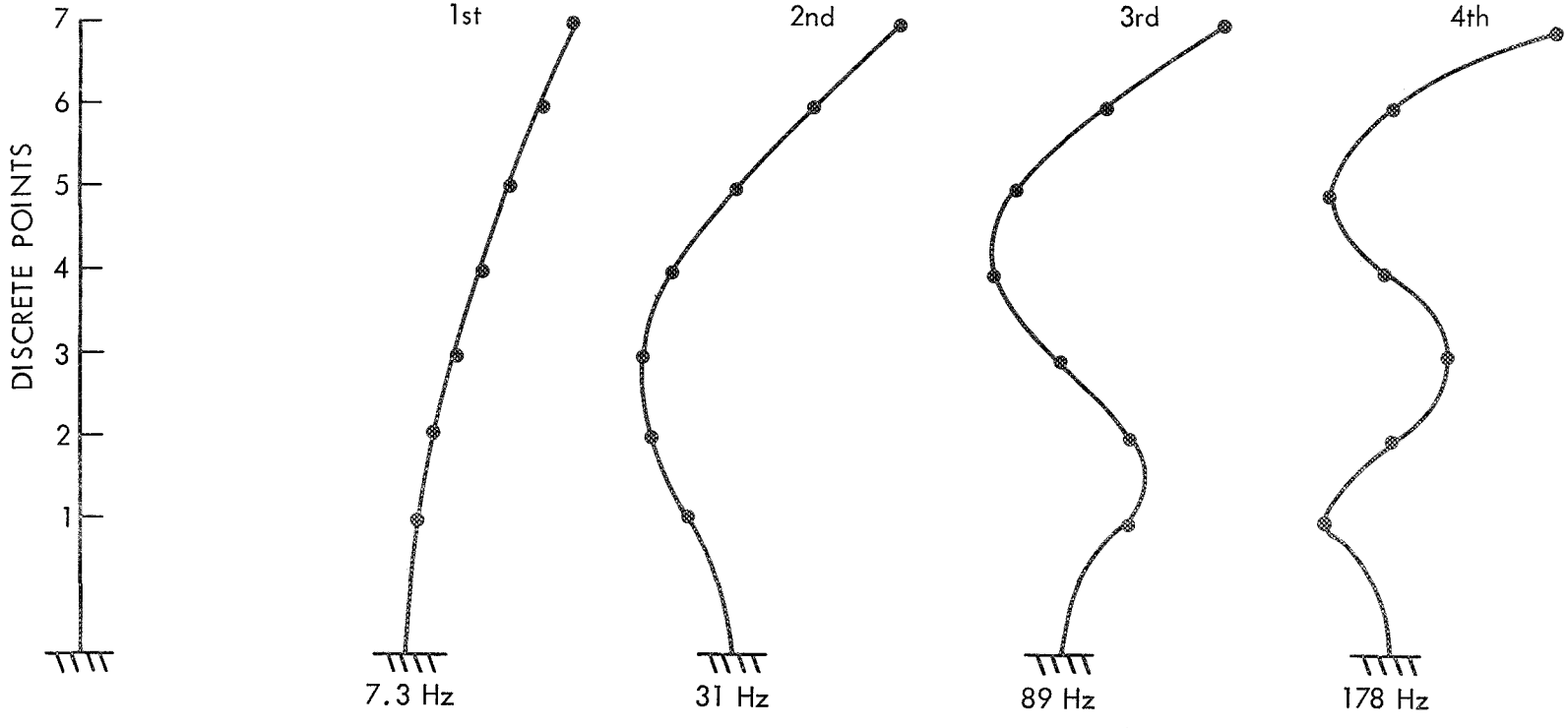

Figure 4. Mode Shapes, Rack only—Nominal Payload Weight with Low C.G.

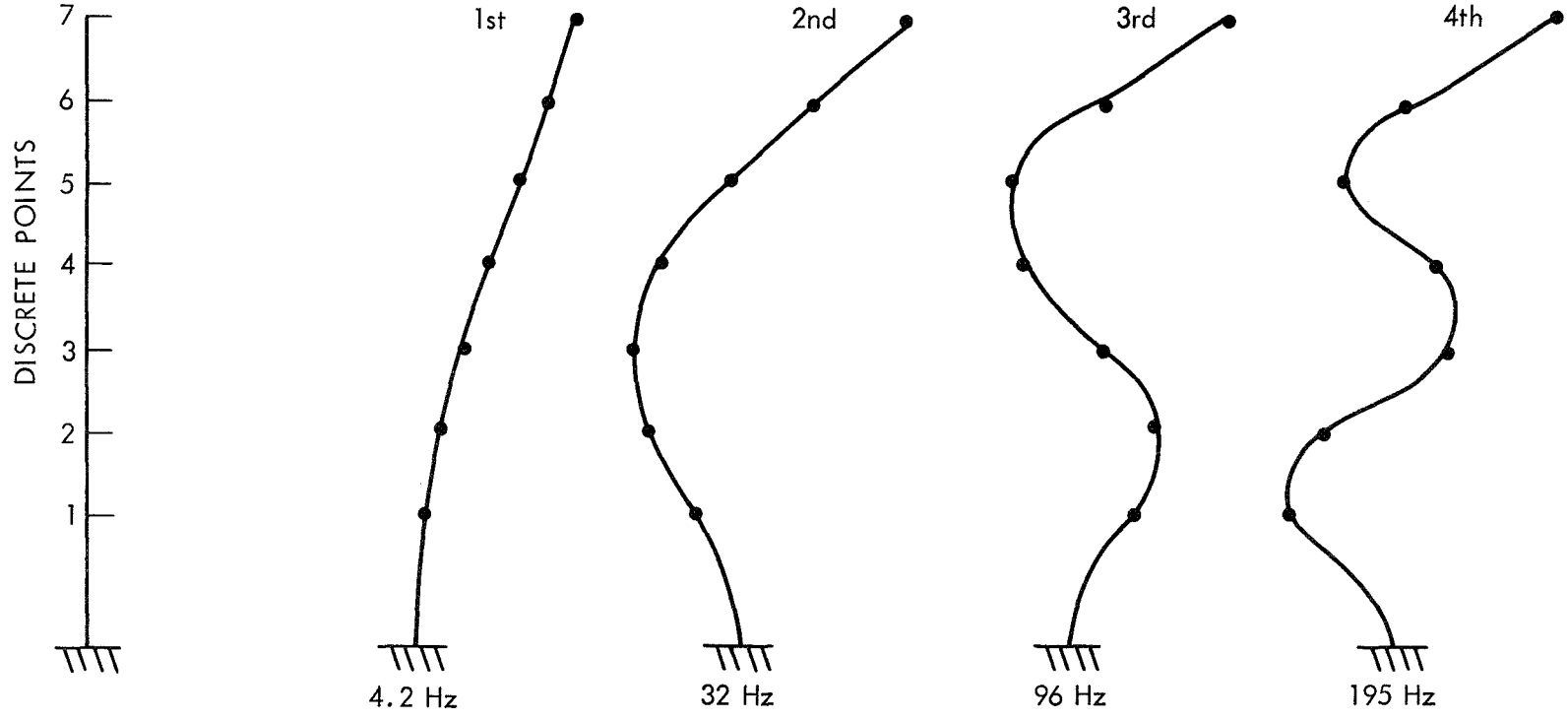

Figure 5. Mode Shapes, Rack only—Nominal Payload Weight with High C.G.

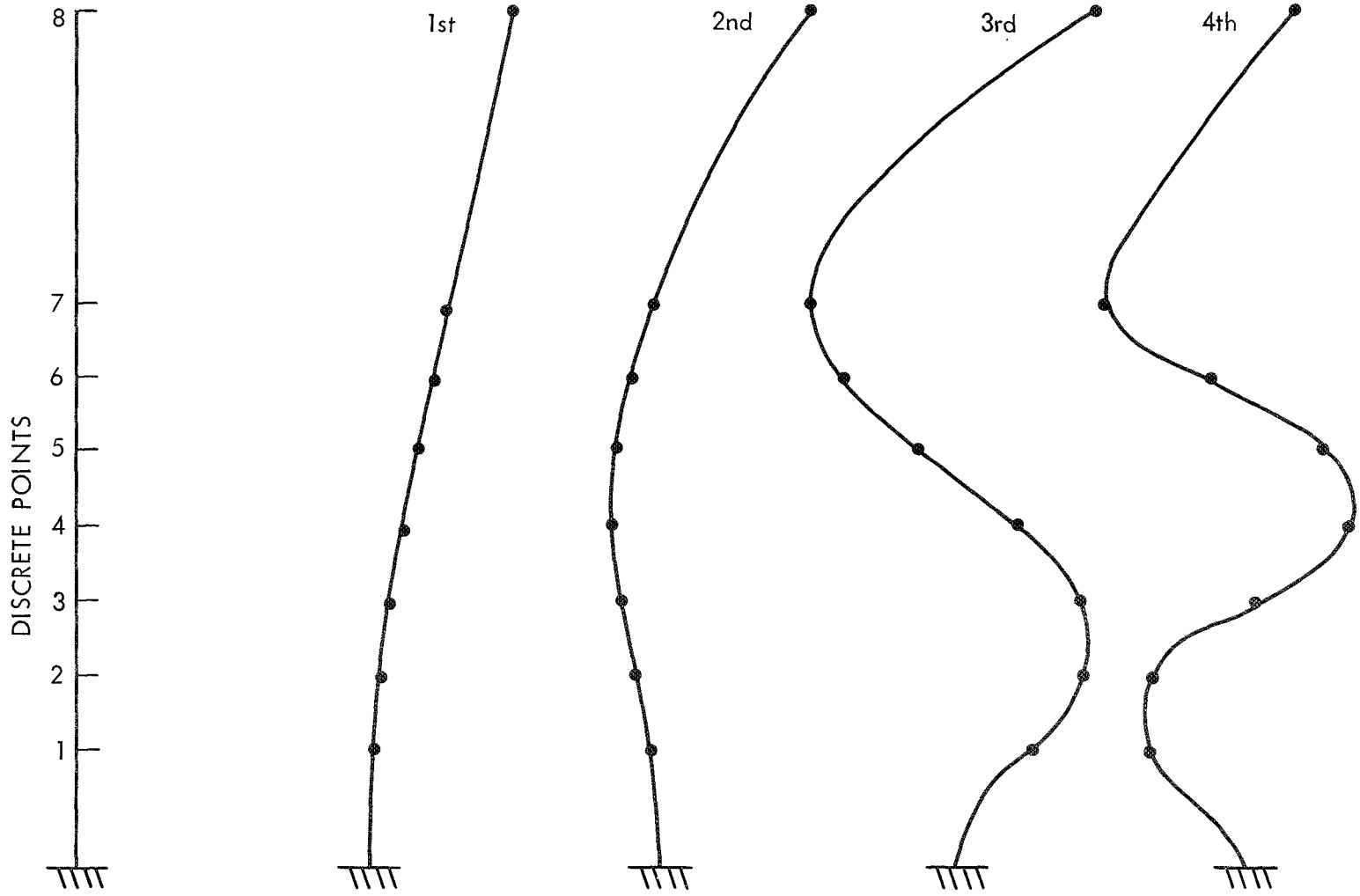

Figure 6. Mode Shapes, Rack/Shroud—Three Uniformly Distributed Payloads (Nominal C.G.)

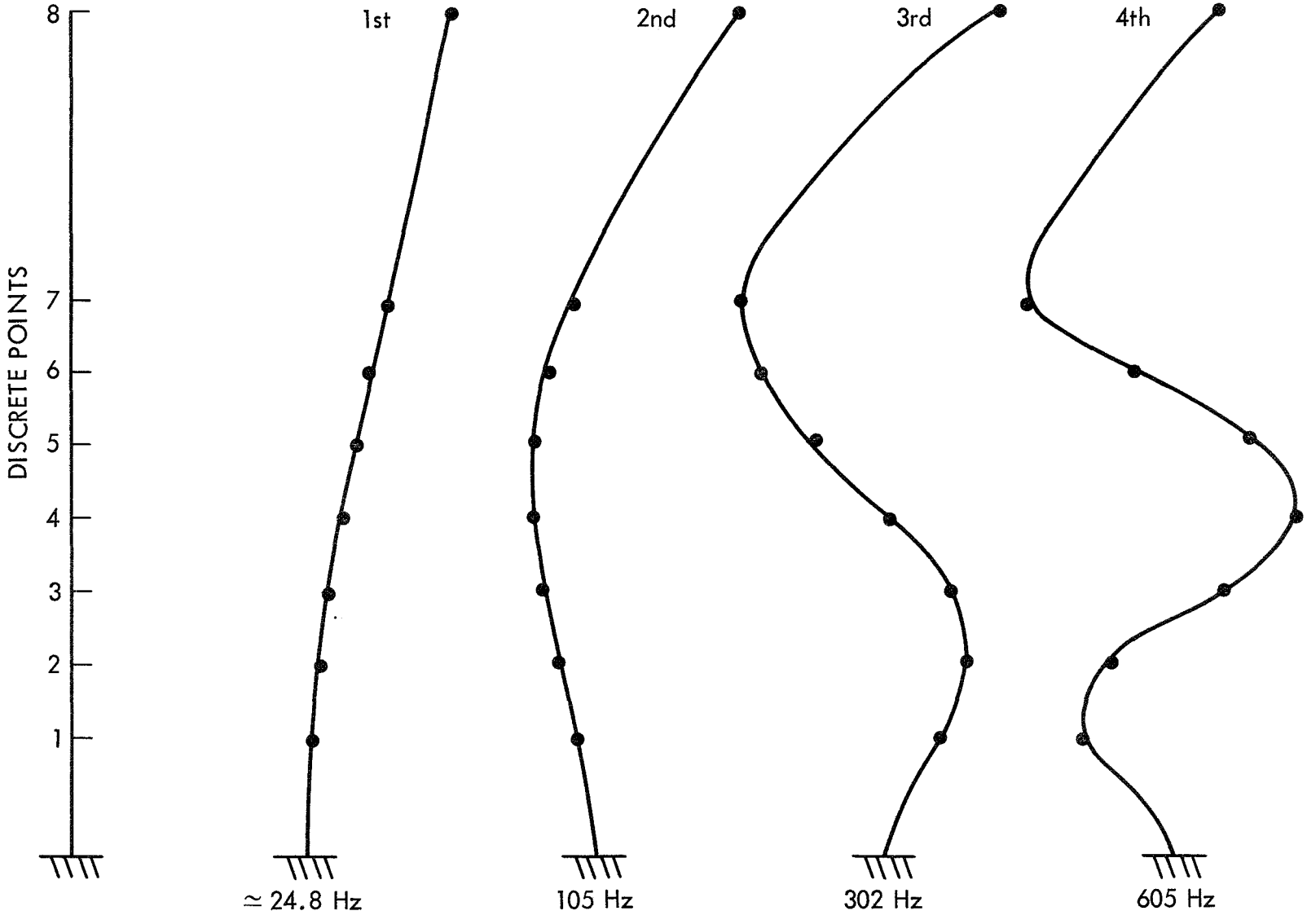

Figure 7. Mode Shapes, Rack/Shroud—Nominal Payload Weight with Low C.G.

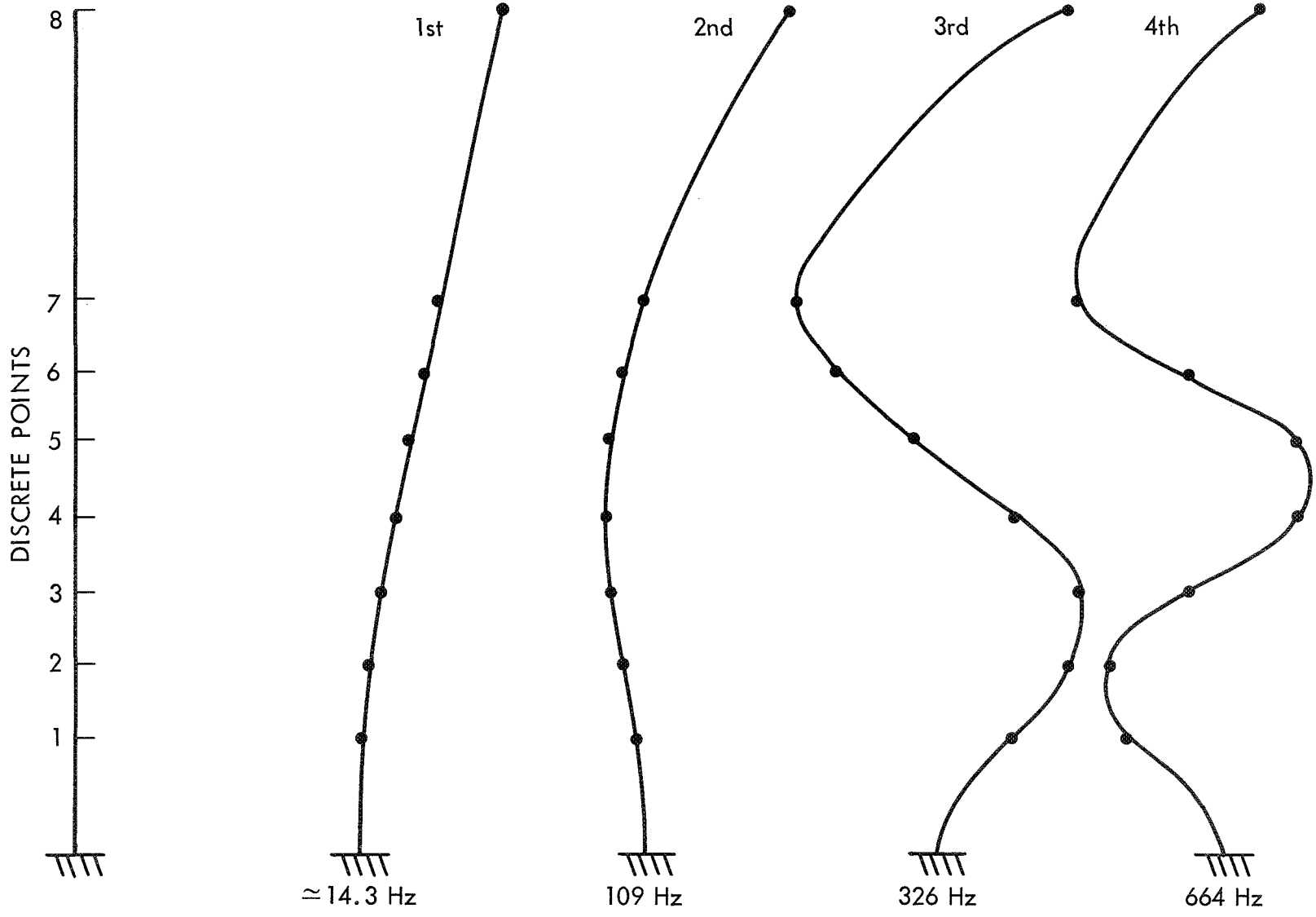

Figure 8. Mode Shapes, Rack/Shroud—Nominal Payload Weight with High C.G.

in the fiberglass shroud. The rack and shroud are bolted together at their bases and are structurally connected at the top of the rack by an o-ring. The longerons, the shelves and the shroud itself are all made of fiberglass. A picture of the rack mounted on the shaker table is shown in Figure 9. The following picture, Figure 10, shows the shroud being slipped down over the rack, while Figures 11 and 12 show the rack/shroud combination in the test configuration for the lateral and thrust axes respectively.

To simulate the mass of a payload, dummy weights were mounted on each shelf. These weights were attached by a 1/2 inch bolt through the centers of the shelves. Accelerometers were located on blocks which were mounted on the longerons directly below each shelf. Accelerometers were also mounted directly on three of the shelves. (This provided a means of correlation between the levels measured on the longerons and the actual levels experienced on the shelves themselves.) Figure 13 shows the accelerometer mountings in detail.

PROCEDURE

A study of this type has many inherent difficulties. Probably the most obvious in this case is that of simulating such a wide range of payload configurations with one test item. Obviously each NIKE APACHE payload is different and will therefore have its own dynamic response. In an effort to simulate a variety of configurations, the two parameters believed to have the greatest effect on the dynamic response of the system were varied—the total weight of the payload and the location of the payload center of gravity. These two parameters were varied one at a time in order to isolate the effect of each on the response of the system.

A compilation of c.g. locations and total weights of previous NIKE APACHE payloads was made. From this list a nominal mass distribution was established. This nominal condition had a total weight of 65 lbs. and a c.g. located 30 inches above the base of the payload. These conditions were satisfied by mounting six lbs. of weights on each shelf. From this list it was also determined over what range the two parameters should be varied. It was originally decided to vibrate five systems with total weights of 53, 59, 65, 71, and 77 lbs. This could be accomplished by uniform distributions with 4, 5, 6, 7, and 8 lbs. on each shelf respectively. (It should be noted that each of these systems has the same c.g. location.) Due to time constraints, only the systems with total weights of 59, 65, and 71 lbs. were tested. It was verified that the majority of payload weights did fall within this range. In a similar manner it was determined that the great majority of payloads have c.g. locations between 25 and 35 inches from the base. These two values together with the nominal value of 30 inches provided three variations for this parameter. (The total weight for each of these

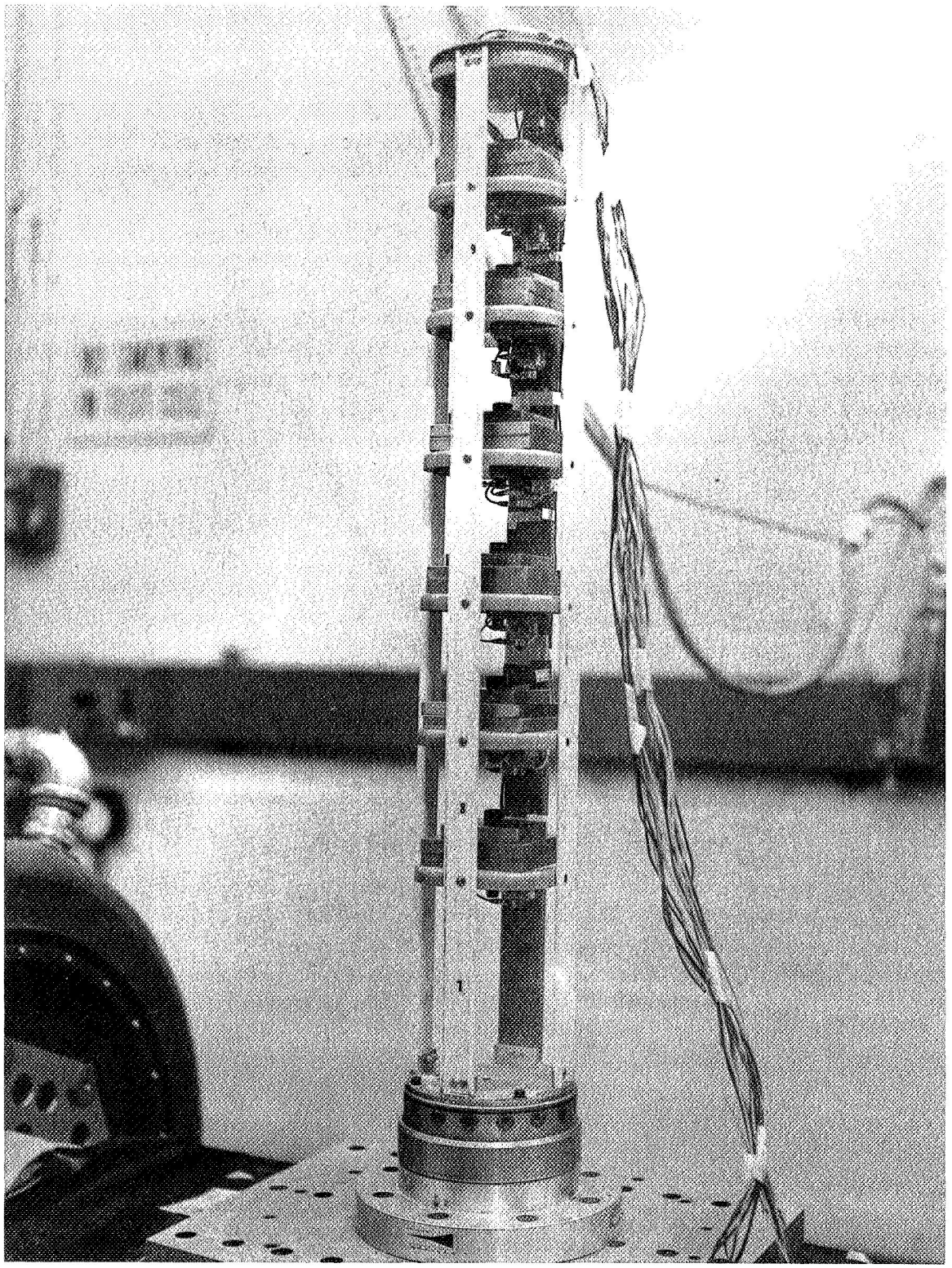

Figure 9. Loaded NIKE-APACHE Payload Rack Mounted on Shaker

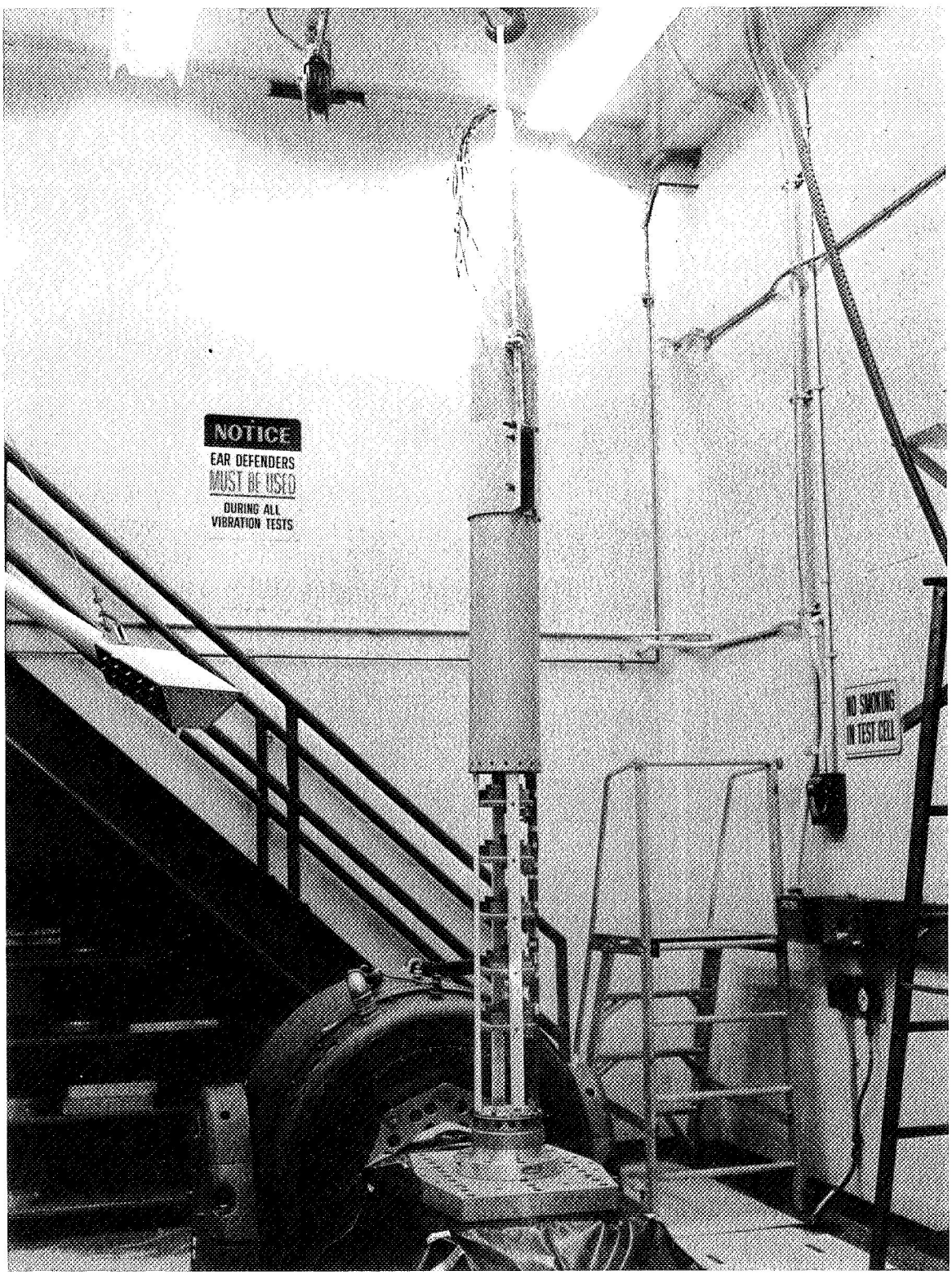

Figure 10. Shroud Being Slipped over Rack

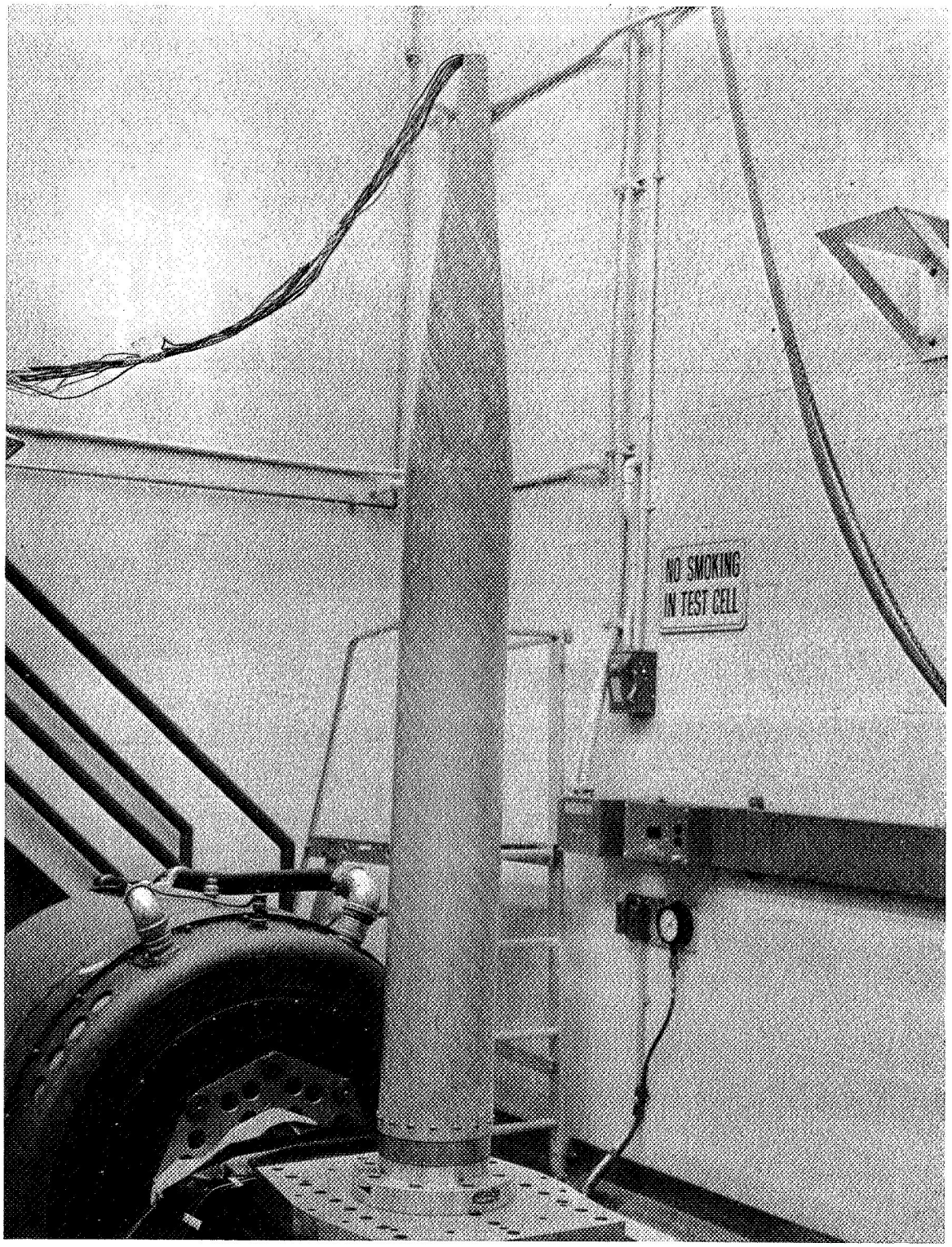

Figure 11. Rack/Shroud Combination in Test Configuration for Lateral Axis

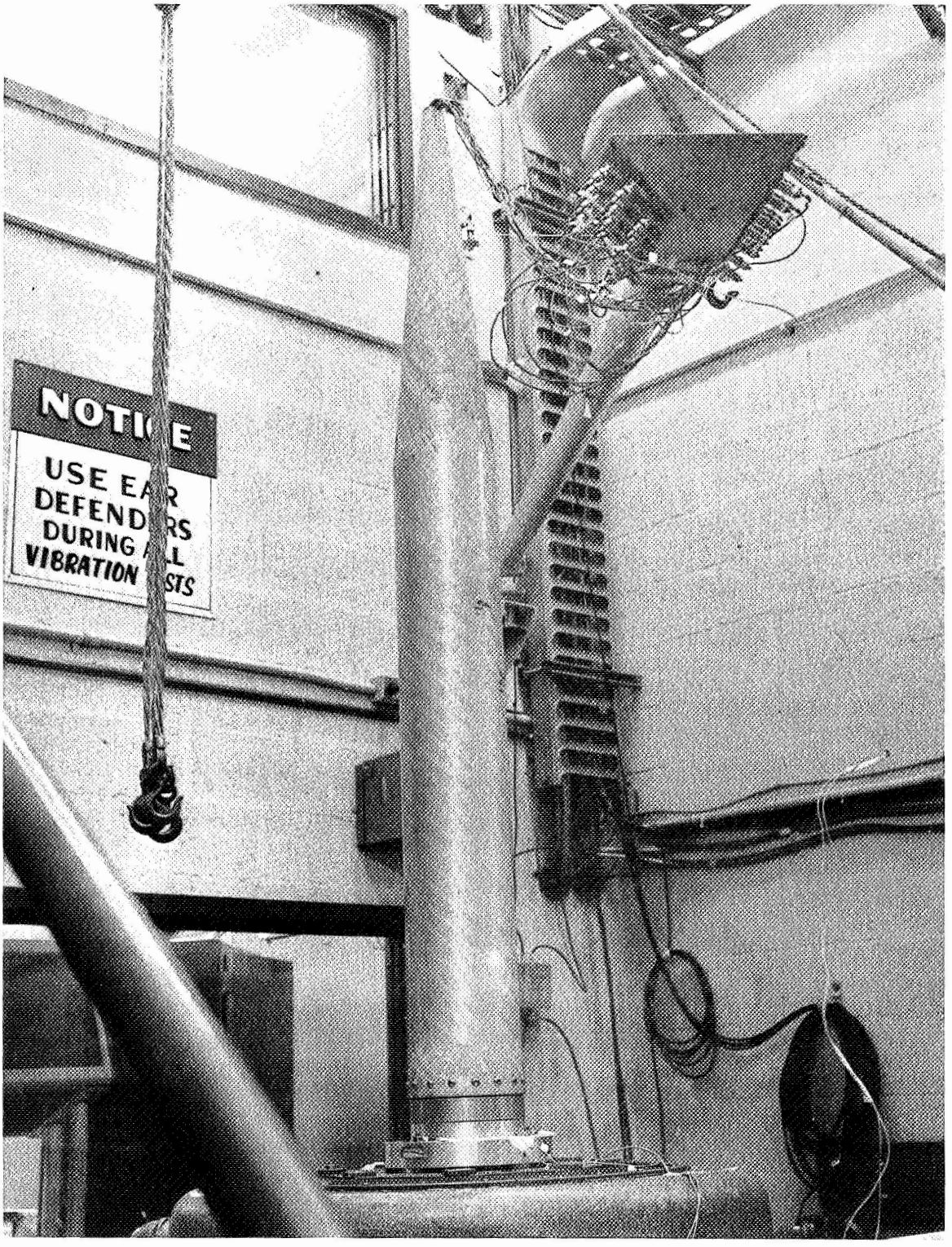

Figure 12. Rack/Shroud Combination in Test Configuration for Thrust Axis

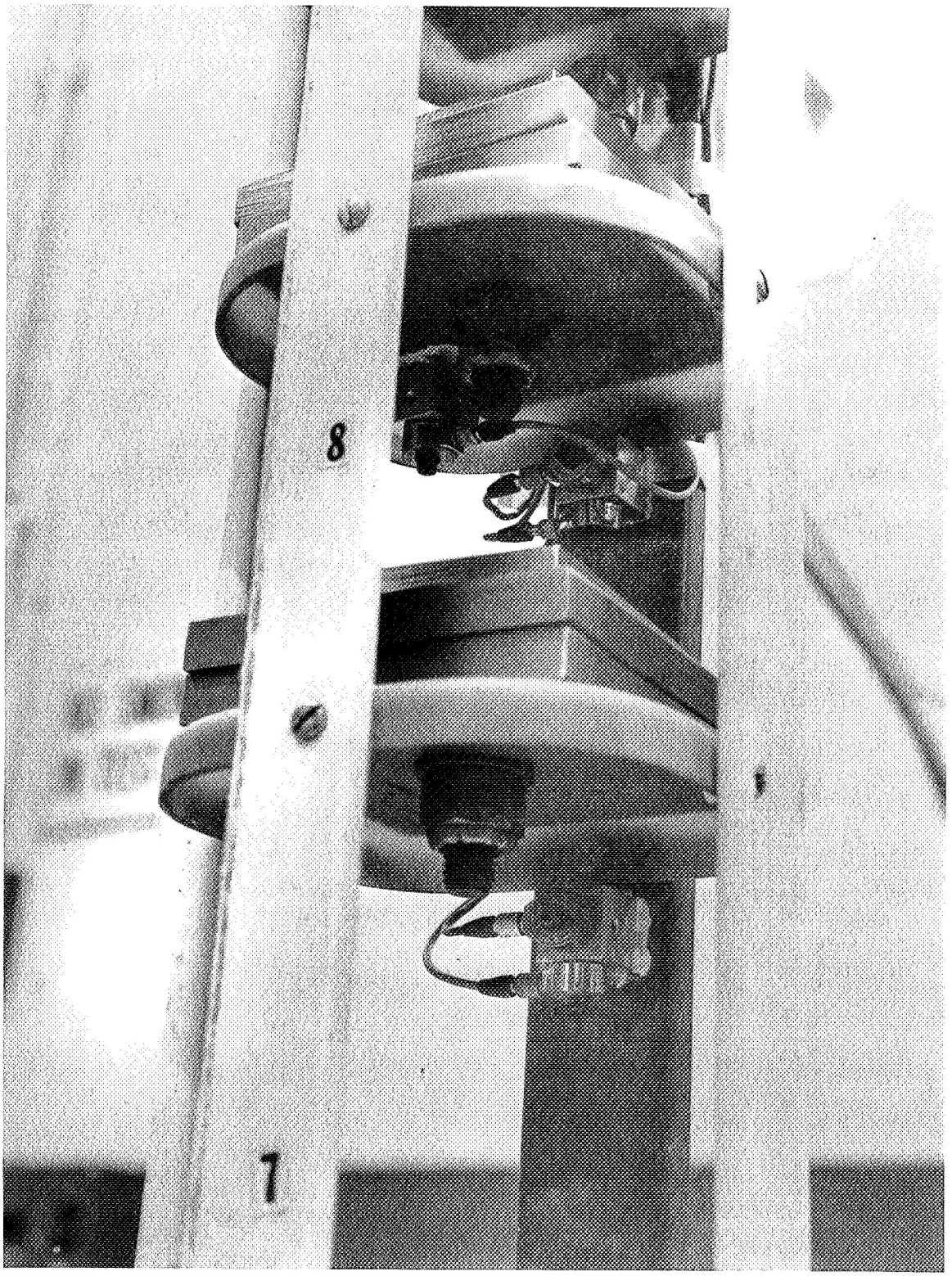

Figure 13. Accelerometer Locations

distributions was 65 lbs.) The previously mentioned variations of the two parameters resulted in a total of five different mass distributions.

It was felt that a more complete knowledge of the rack/shroud dynamic response could be obtained if the response of the rack alone were first determined. Hence, before the loaded rack/shroud combination was exposed to vibration, the loaded rack was vibrated alone. For each of the five mass distributions, the rack was exposed to sinusoidal frequency sweeps (4 octaves/min from 5 to 2000 Hz) of intensity 1 g, once along the thrust axis and once along each of the two lateral axes. The results of these runs will not be presented in detail here, but their general nature will be discussed in the final section of this report.

The system was then vibrated in the rack/shroud configuration. It was decided to vibrate this configuration along only one lateral axis since the results for the two lateral axes of the rack were practically identical. The rack/shroud configuration was subjected to a lateral sine sweep of 1 g from 10 to 30 Hz and 2 g's from 30 to 2000 Hz; along the thrust axis the level was a constant 2 g's. This sequence was performed for each of the five mass distributions. From each run a plot of peak acceleration vs. frequency was obtained for every accelerometer on the shake axis.

Each mass distribution in the rack/shroud configuration was also subjected to a decaying sinusoidal shock transient of 10 g's (0 to peak) at a frequency of 136 Hz along the thrust axis. The nominal mass distribution was also subjected to a spec level sine sweep and a 5 g-rms random input in both axes. The data from these random runs was analyzed and Power Spectral Density plots obtained.

RESULTS

Low Level Sweeps on Nominal Condition

As was previously stated, the input along the lateral axis was 1 g from 10 to 30 Hz and 2 g's from 30-2000 Hz. There were four distinct regions where amplification of the input took place. Figure 14 presents a plot of peak accelerations vs. frequency for the response at the second shelf. The largest amplification took place in the frequency region from 15-23 Hz. (This corresponds to the predicted natural frequency of 17 Hz.) The greatest amplification Q (here Q = response level/input level) measured on any of the shelves was measured at the second shelf, while the remaining shelves all experienced amplifications as high as 9. The second largest amplification occurred in the frequency range from 40 to 60 Hz with a Q max. = 3.5. The third resonance occurred from 110 to 170 Hz with a Q max. = 5.0, and the last lateral resonance took place from 370 to 570 Hz with a Q max. = 3.0.

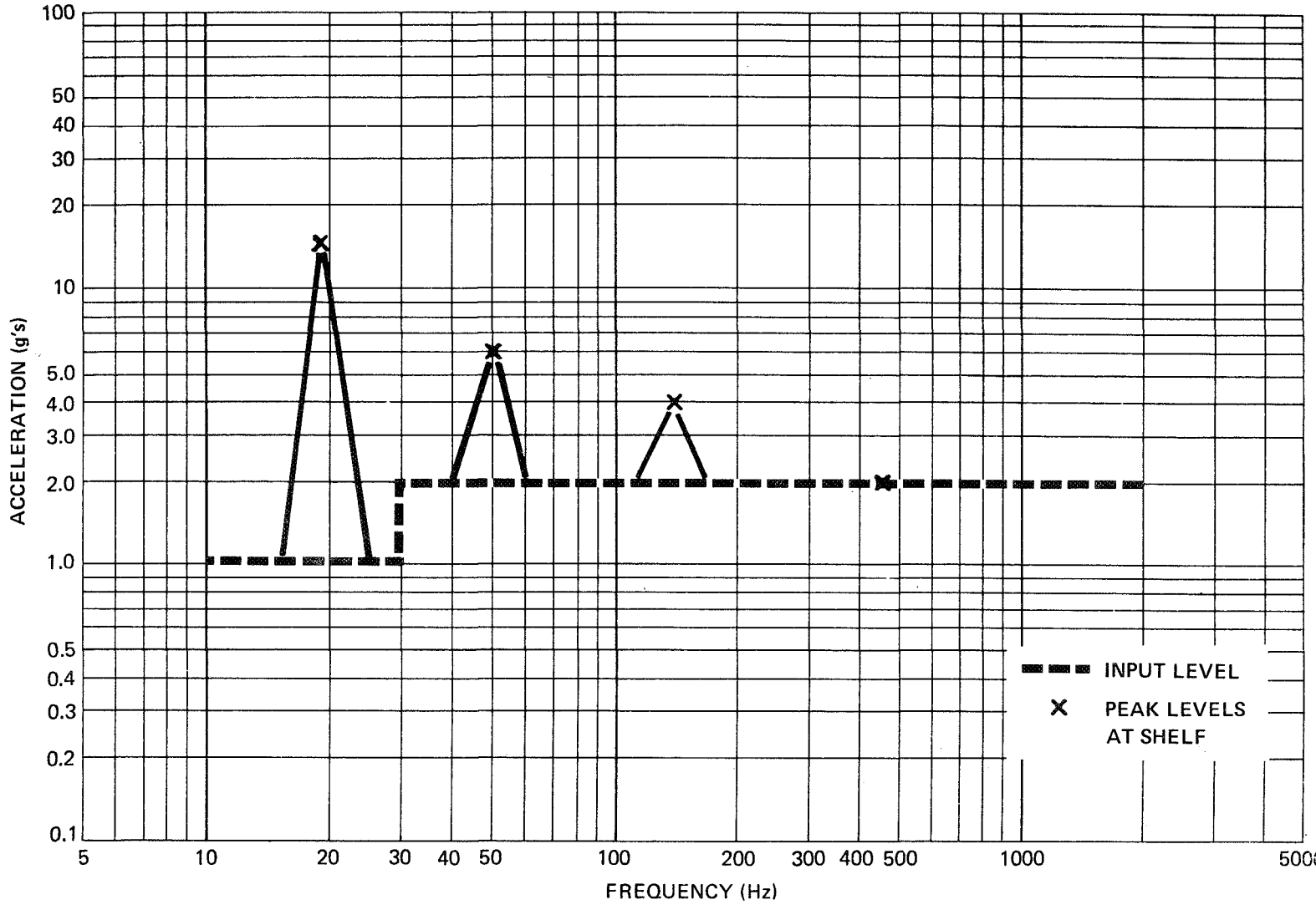

Figure 14. Frequency Response, at 2nd Shelf, of the Nominal Payload Distribution to Lateral Vibration

In the thrust axis there were only two frequency regions where amplifications of the input were detected. However, these amplifications were more severe than in the lateral axis and occurred at fairly high frequencies. The response at the top shelf is shown in Figure 15. The first resonance occurred from 65 to 105 Hz and produced a Q = 25 on most of the shelves. The second resonance took place in the frequency range from 370 to 510 Hz with applifications as high as Q = 20. These two resonant frequencies correspond to the theoretical predictions of the natural frequencies of the loaded shelves and the four longerons.

From the data obtained from the sine sweeps it would be difficult to arrive at any conclusion concerning the relationship between shelf location and the degree of amplification of the input level.

Variation of Payload Wt.

To determine the effect of the payload total weight on the dynamic response of the system, three uniform mass distributions with different total weights were employed, as mentioned above. The nominal condition had 6 lbs. mounted on each shelf, for a total weight of 65 lbs. To deviate from the nominal condition two other arrangements were used, one with 7 lbs. on each shelf (total wt. = 71 lbs.) and the other with 5 lbs. on each shelf (total wt. = 59 lbs.).

When the dynamic responses of these three systems are compared, for identical inputs, they are found to be quite similar. Figure 16 shows the responses, at the bottom shelf, of the three systems to the same lateral input (1 g at 10-30 Hz, 2 g's at 30-2000 Hz). The greatest variation in the magnitudes of the responses occurred at this particular shelf. A similar comparison was made of the responses at each of the other shelves. From this series of comparisons the following observations were made:

1) As would be expected, the four regions of amplification tend to occur at increasingly higher frequencies as the total weight of the system decreases.

2) The frequency ranges where amplifications take place tend to widen as the total weight is increased.

3) Variation in payload total weight did not produce significant variations in the magnitude of the induced responses.

A corresponding set of comparisons was made among the responses of the three systems to identical thrust axis inputs (2 g's at 10-2000 Hz). Figure 17 compares the thrust axis responses at the top shelf. As can be seen, the responses are almost identical. This also proved to be the case for the remaining

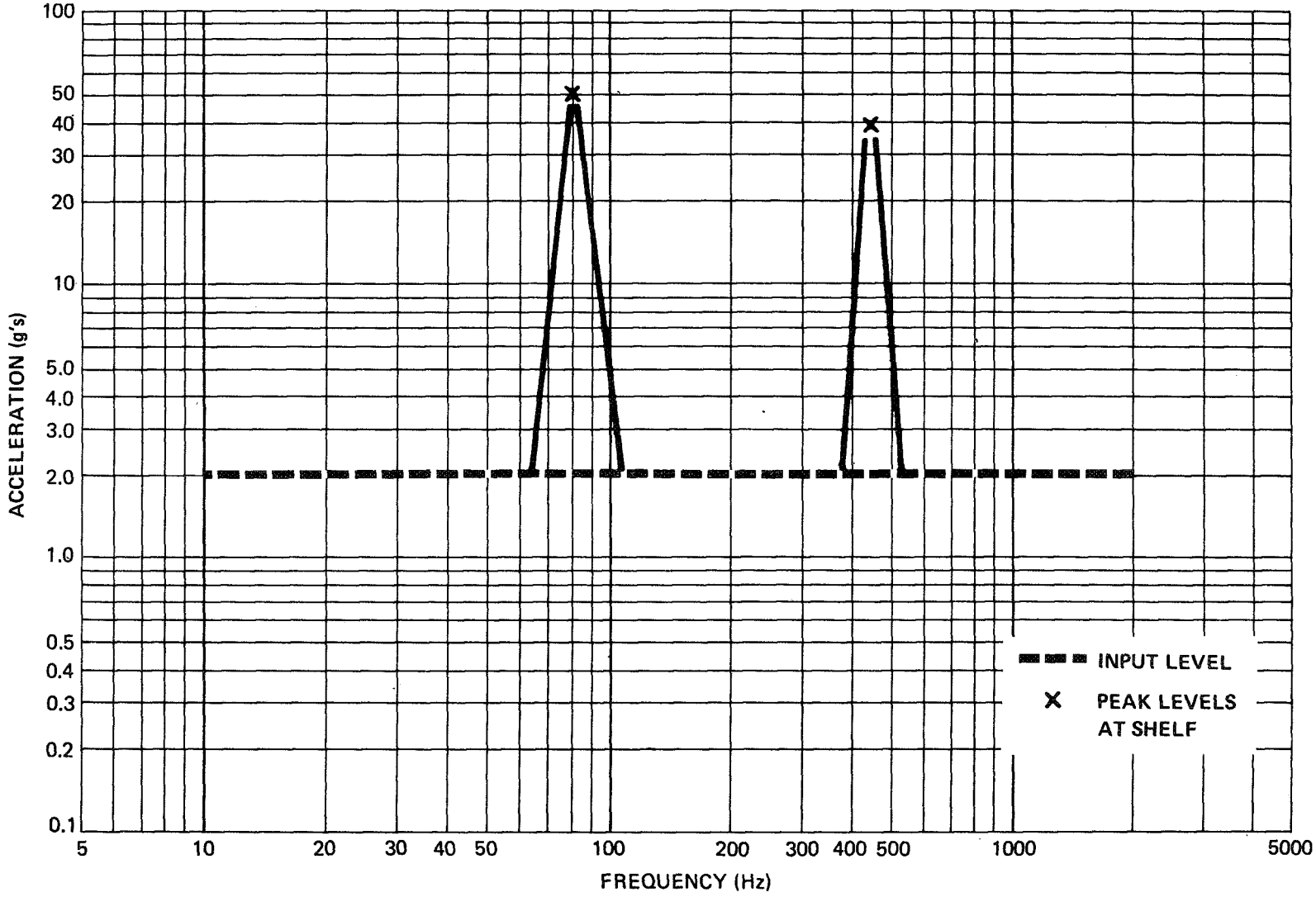

Figure 15. Frequency Response, at Top Shelf, of the Nominal Payload Distribution to Thrust Axis Vibration

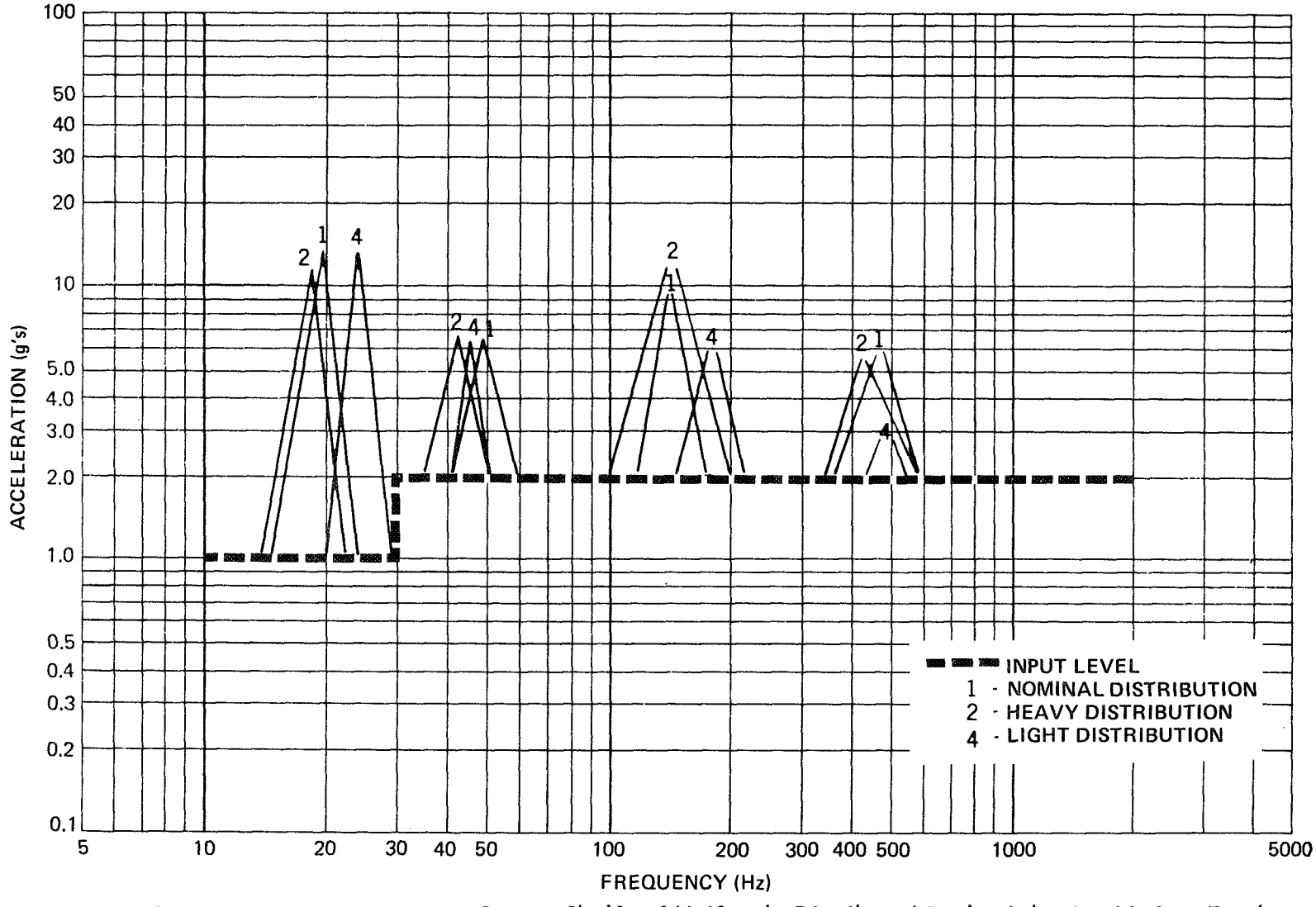

Figure 16. Frequency Response, at Bottom Shelf, of Uniformly Distributed Payloads having Various Total Weights to Lateral Vibration

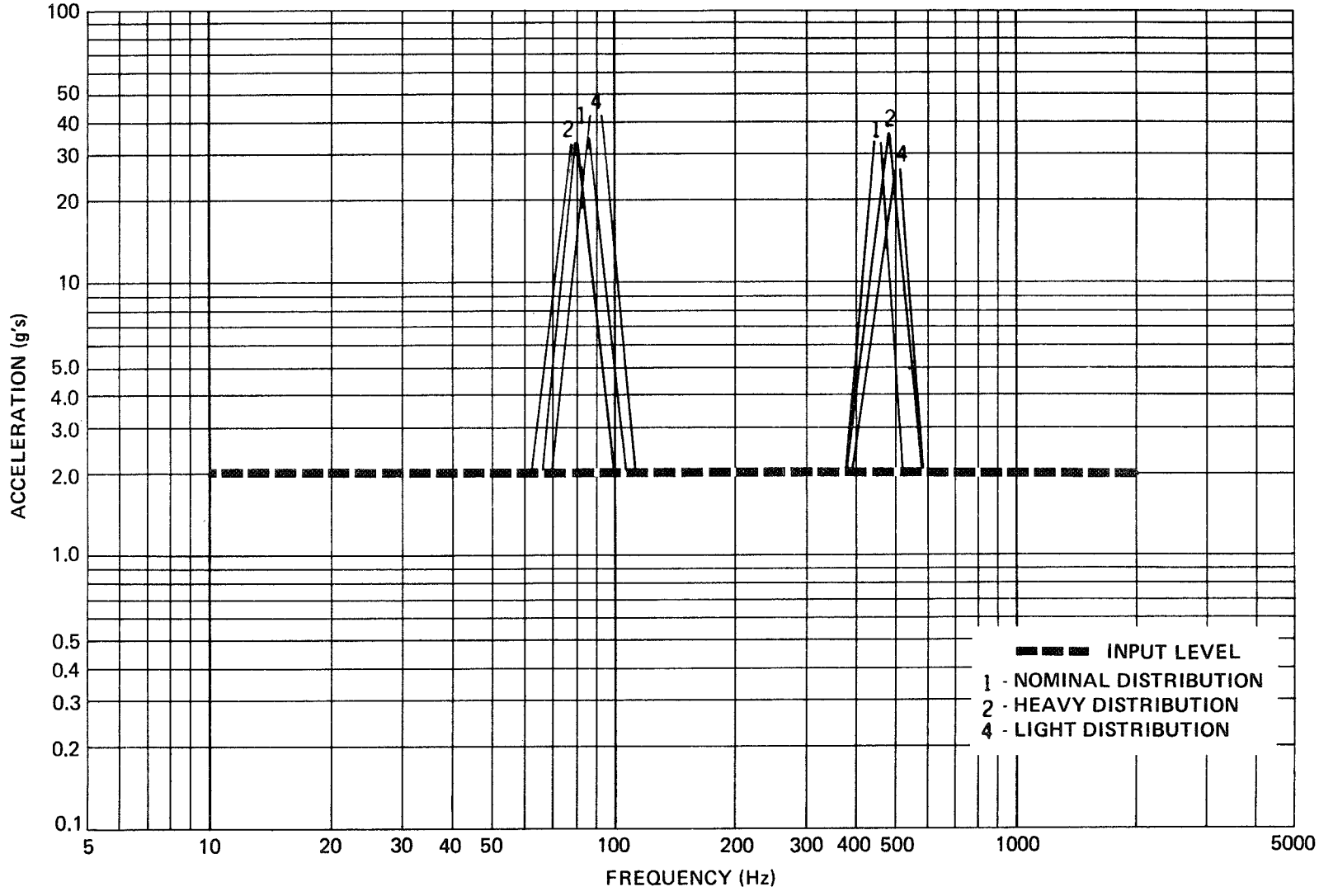

Figure 17. Frequency Response, at Top Shelf, of Uniformly Distributed Payloads having Various Total Weights to Thrust Vibration

shelves. Therefore, it was concluded that a variation in the total weight does not appreciably affect the system response to an input in the thrust axis.

Variation of Payload C.G. Location

By distributing a given total payload weight among the shelves in various ways, the c.g. of the system could be placed at any desired position. To determine the effect on the system response produced by this variable, three different payload distributions were employed. One was the nominal distribution, which had a c.g. location 30 inches above the base of the rack. The other two distributions had c.g. locations of 25 and 35 inches above the base of the rack. (Each of these mass distributions had the same total weight of 65 lbs.)

The results of the lateral axis vibration tests will be considered first. Figure 18 shows the responses, measured at the bottom shelf, of the three distributions to identical lateral inputs (1 g 10-30 Hz, 2 g's 30-2000 Hz). From this plot it is apparent that the distribution with the lowest c.g. had the greatest degree of amplification at the first two resonances. This was found to be the case at all of the shelf locations. Similarly, the nominal distribution exhibited a somewhat greater amplification at the first two resonances than did the system with the highest c.g. This trend tends to indicate that the degree of amplification at the resonances increases as the c.g. is lowered. However, at the other two resonant points there were no consistent differences between the responses of the three systems. Surprisingly, the frequency ranges of amplification did not vary appreciably for the three distributions.

In the thrust axis the system response was not noticeably affected by the variation in c.g. location. Figure 19 shows the responses, measured at the top shelf, of the three set-ups to identical inputs (2 g's at 10-2000 Hz). The responses are almost identical, as was the case at the other shelves.

Spec Level Sine Vibration

After the various mass distributions were exposed to low-level frequency sweeps, the nominal distribution was exposed to spec level sinusoidal vibration, both in the thrust axis and in one lateral axis. Since the previous testing had provided a basic knowledge of the effects of varying the mass and c.g. location, it was felt that for this test it was adequate to use the nominal mass distribution only. (This decision was also affected somewhat by facility and time constraints.)

The specifications for the sinusoidal vibration of the NIKE-APACHE are included in Table 1.

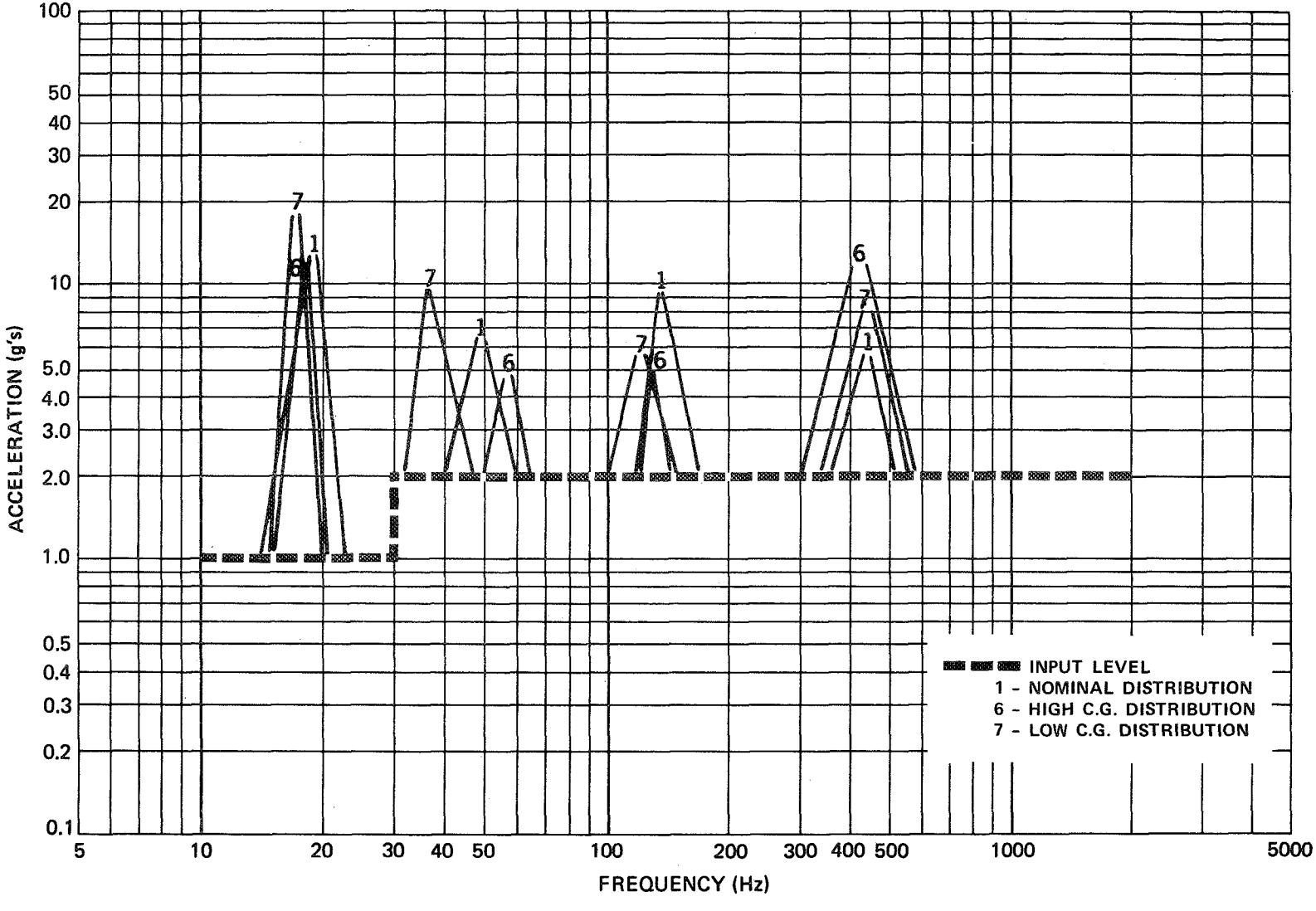

Figure 18. Frequency Response, at Bottom Shelf, of Various Payload Distributions having Different C.G. Locations to Lateral Vibration

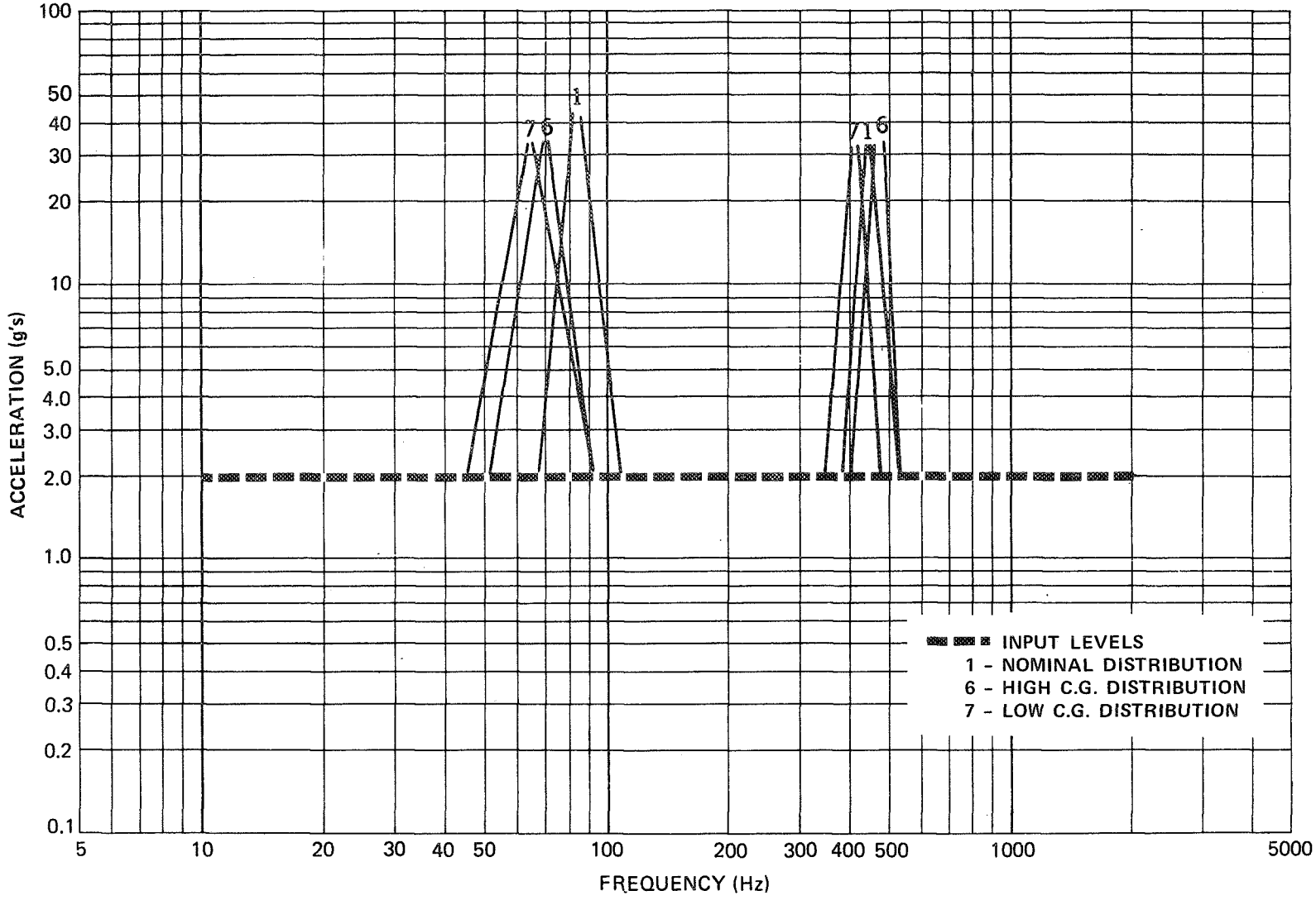

Figure 19. Frequency Response, at Bottom Shelf, of Various Payload Distributions having Different C.G. Locations to Thrust Vibration

Table 1
Present NIKE-APACHE Sinusoidal Vibration Specifications

Axis	Frequency Range (Hz)	Level (g, 0-to-peak)	Sweep Rate
Thrust z-z	10-120 120-300 300-400 400-2000	3.0 7.0 10.0 5.0	4 Octaves per minute
Lateral X-X and Y-Y	7-30 30-40 40-120 120-2000	1.0 2.0 0.024" D.A. 5.0	4 Octaves per minute

Random

Axis	Frequency Range (Hz)	PSD Level (g^2/Hz)	Acceleration (g-rms)	Duration
Thrust z-z	20-2000	0.20	20.0	10 sec.
Lateral X-X and Y-Y	20-2000	0.20	20.0	10 sec. per axis

Sinusoidal Transient

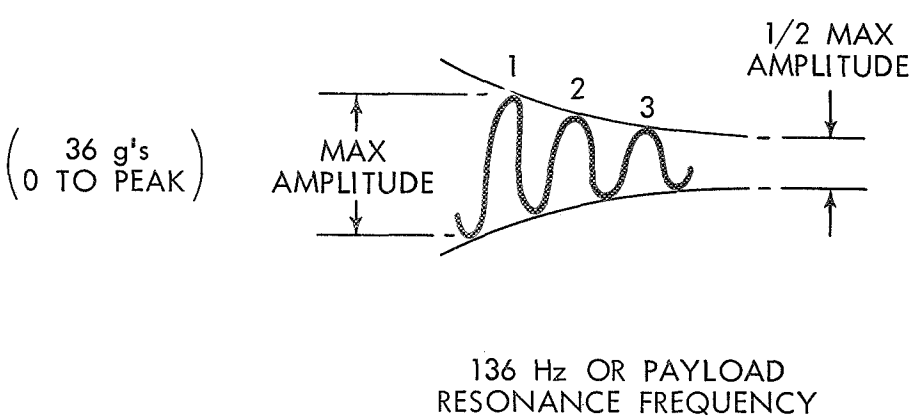

The response to the lateral input will first be discussed. Figure 20 presents the response recorded at the top shelf. Similar plots for the responses at the other shelves were also drawn. As with the low level sweeps, there were four frequency ranges where amplification of the input occurred. The first of these was at the fundamental frequency of the system, where the results were the same as those obtained from the low level sweeps. The reason for this was that the input levels of the two runs were the same at low frequencies (less than 30 Hz). From 40-120 Hz the specification calls for an input of 0.024" DA (constant displacement). This produces an acceleration level of 18 g's at 120 Hz. If a payload resonance takes place near this region, extremely high induced responses may occur. The highest level recorded at 120 Hz was a reading of 60 g's (Q = 33) at the bottom shelf. This was by far the highest response measured in the lateral axis at any frequency. As can be seen from Figure 20 the response at the top shelf reached a level of only 25 g's or Q = 1.4. Above 120 Hz the spec calls for a constant acceleration of 5 g's. Two resonance points were encountered above this frequency, both of which yielded a maximum amplification of 4 or a peak acceleration of 20 g's. The majority of the peak responses at these points were in the neighborhood of 10 g's.

In the thrust axis the largest amplifications took place at the first resonance point (60-100 Hz). The highest response was a peak acceleration of approximately 60 g's (Q = 20) measured at the bottom shelf (see Figure 21). The rest of the shelves all experienced responses in the neighborhood of 50 g's (Q = 17) at the first resonance. Another region of high amplification occurred around 500 Hz where the input level was 5 g's. A peak level of 60 g's (Q = 12) was recorded at the top shelf.

These were the only two resonances which were detected during the low level sweeps. (The full scale settings for the read-out were set at 100 g's to prevent clipping at the two resonance points just mentioned.) However, from the spec level results two intermediate regions of lesser amplification were detected. From 120-200 Hz the spec calls for an input of 7 g's. Response levels of 25 g's (Q = 3.6) were measured in this region. In the frequency range from 300-400 Hz the input was a constant acceleration of 10 g's. Responses as high as 60 g's (Q = 6) were measured in this region.

After the responses from the spec level run were evaluated a correlation was made with the data obtained from the low-level sweeps. In the lateral axis, the response of the system was very nearly linear (i.e., amplification of the input was nearly independent of the input level). However, in the thrust axis the system response was not as linear; the degree of amplification was less when the input level was increased. For example, during the low level sweep (input of 2 g's), peak levels of 40 g's were measured at the top two shelves at 500 Hz

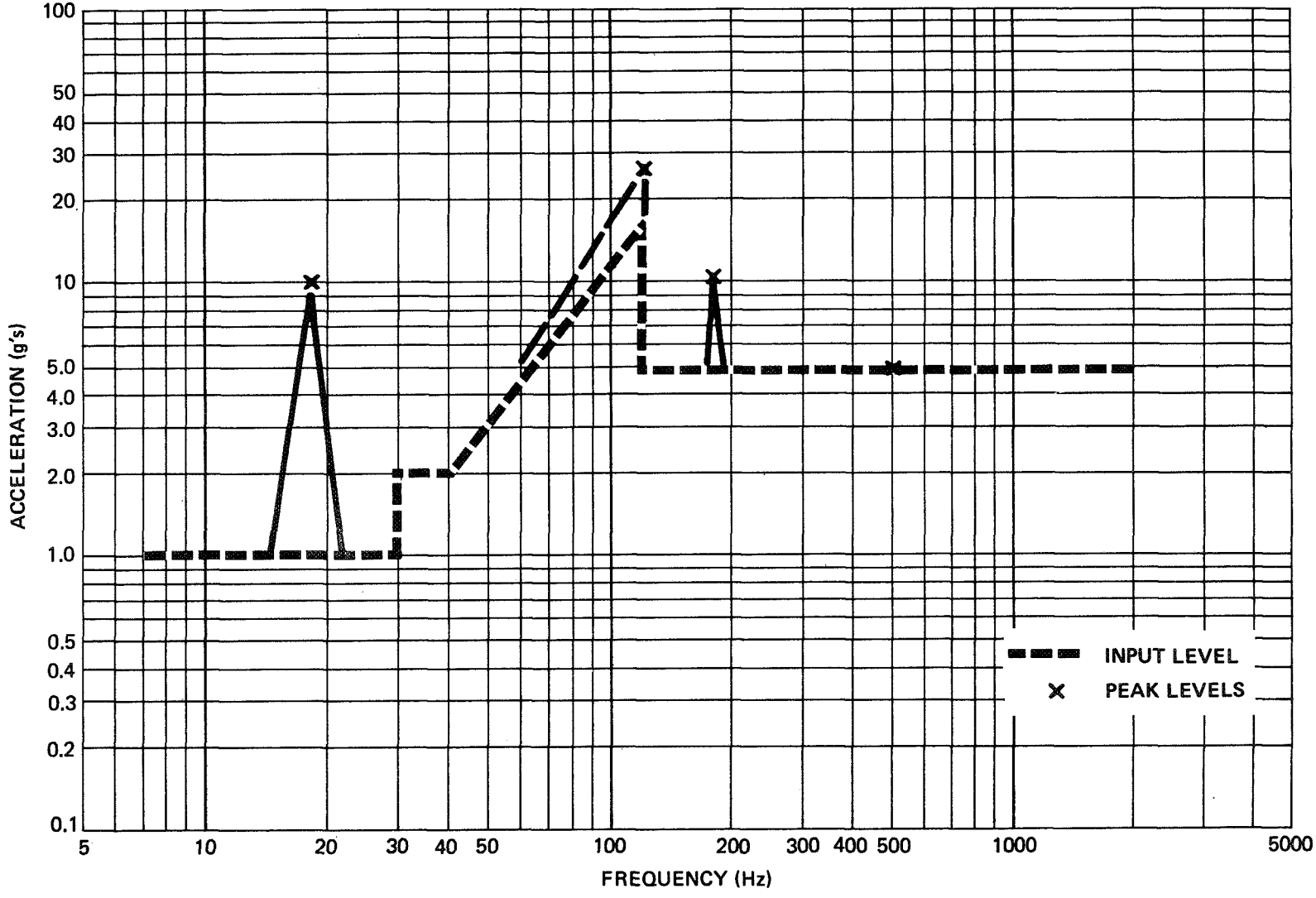

Figure 20. Frequency Response, at Top Shelf, of Nominal Distribution to Lateral Spec Input

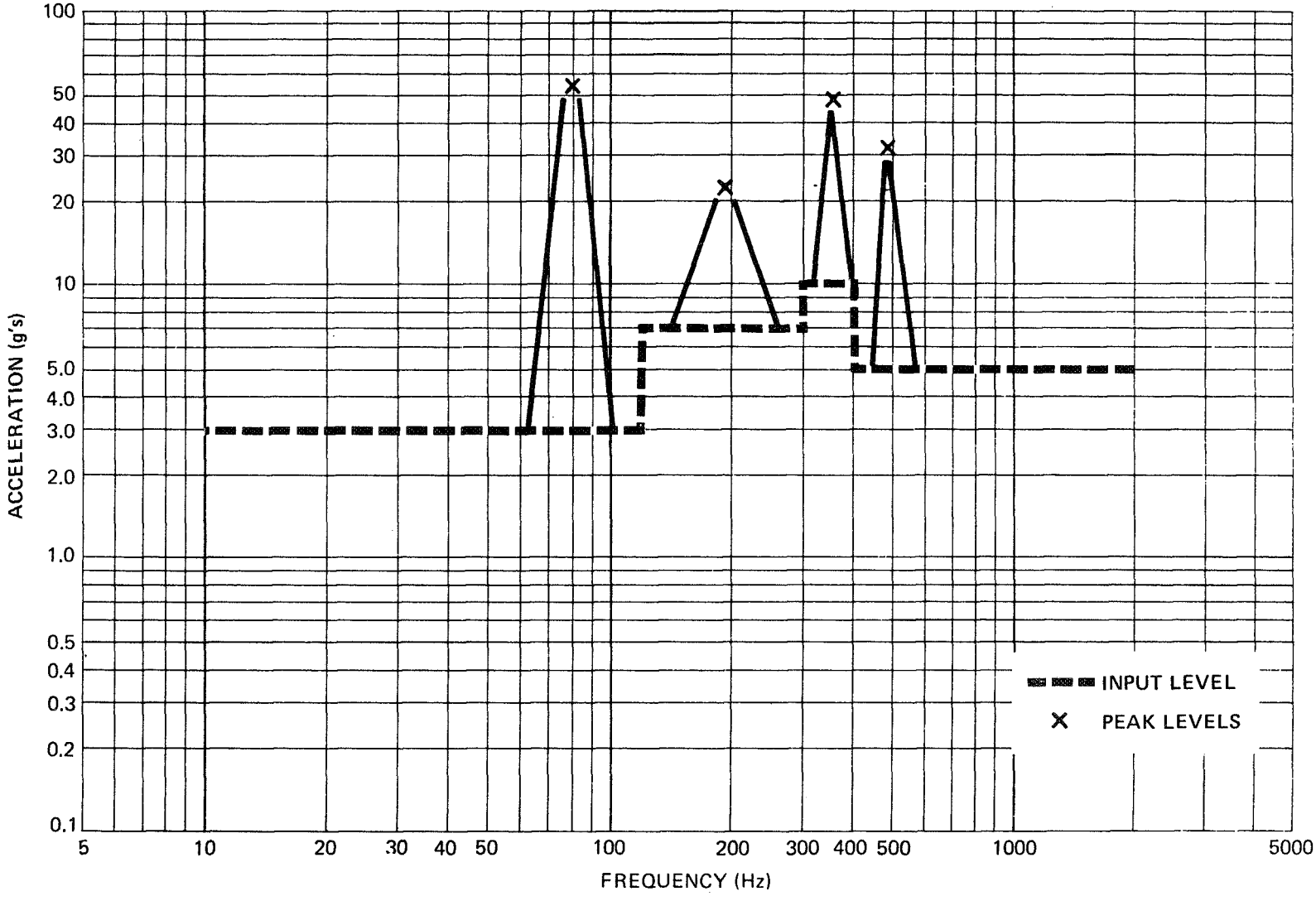

Figure 21. Frequency Response, at Bottom Shelf, of Nominal Distribution to Thrust Axis Spec Input

(this yields Q = 20). The corresponding peak acceleration during the spec run at these shelves was 60 g's. For a 5 g input this gives Q = 12 (as compared to Q = 20 for the low level sweeps). This phenomenon was detected at almost all the shelves in the two regions of highest amplification.

Random Vibration

It was felt that some knowledge of the system (nominal distribution) response to a random input should be obtained. The NIKE-APACHE random vibration specification (see Table 1) calls for a random input of 20 g's rms for 10 seconds, with a flat spectrum from 20 to 2000 Hz, in the thrust and two lateral axes. The test item was exposed to a level of 5 g's rms for 10 seconds in the thrust and one lateral axis. Power Spectral Density (PSD) plots were made of the response at each shelf to thrust axis and lateral axis inputs. The resulting PSD plots of the response at the top shelf are shown in Figures 22 and 23 respectively. The over-all levels of the responses during thrust vibration were generally about 15 g's rms. During lateral vibration the over-all levels were generally about 3 g's rms.

Sinusoidal Shock Transient

In addition to sine and random vibration, the NIKE-APACHE test spec calls for a decaying sinusoidal shock transient (36 g's 0 to peak) in the thrust axis (see Table 1). This shock simulates the payload's response to first stage ignition. The frequency of this shock is tuned to the resonant frequency of the payload (if it falls in the range of 120-150 Hz) or at 136 Hz if a resonance doesn't fall in the specified region. Each of the previously described mass distributions was subjected to such a shock but of lower magnitude (10 g's 0 to peak). The response to this shock was measured and recorded at each shelf. The responses measured at all shelves for each distribution consistently reached 30 g's, or an amplification of 3.

Correlation of Test Results with Theoretical Predictions

At this time some general remarks concerning this study will be made. When correlating the theoretical predictions with the experimental results it was noticed that the data from the rack only agreed very well with the theoretical predictions. This can best be shown by a comparison of the predicted mode shapes and the actual mode shapes obtained from the test results. (These latter mode shapes were obtained by normalizing the peak accelerations at the four frequencies of amplification.) Such a comparison for the set-ups with uniform mass distributions is presented in Figure 24. It is easily seen that the experimental results are almost identical to the theoretical prediction. This indicates

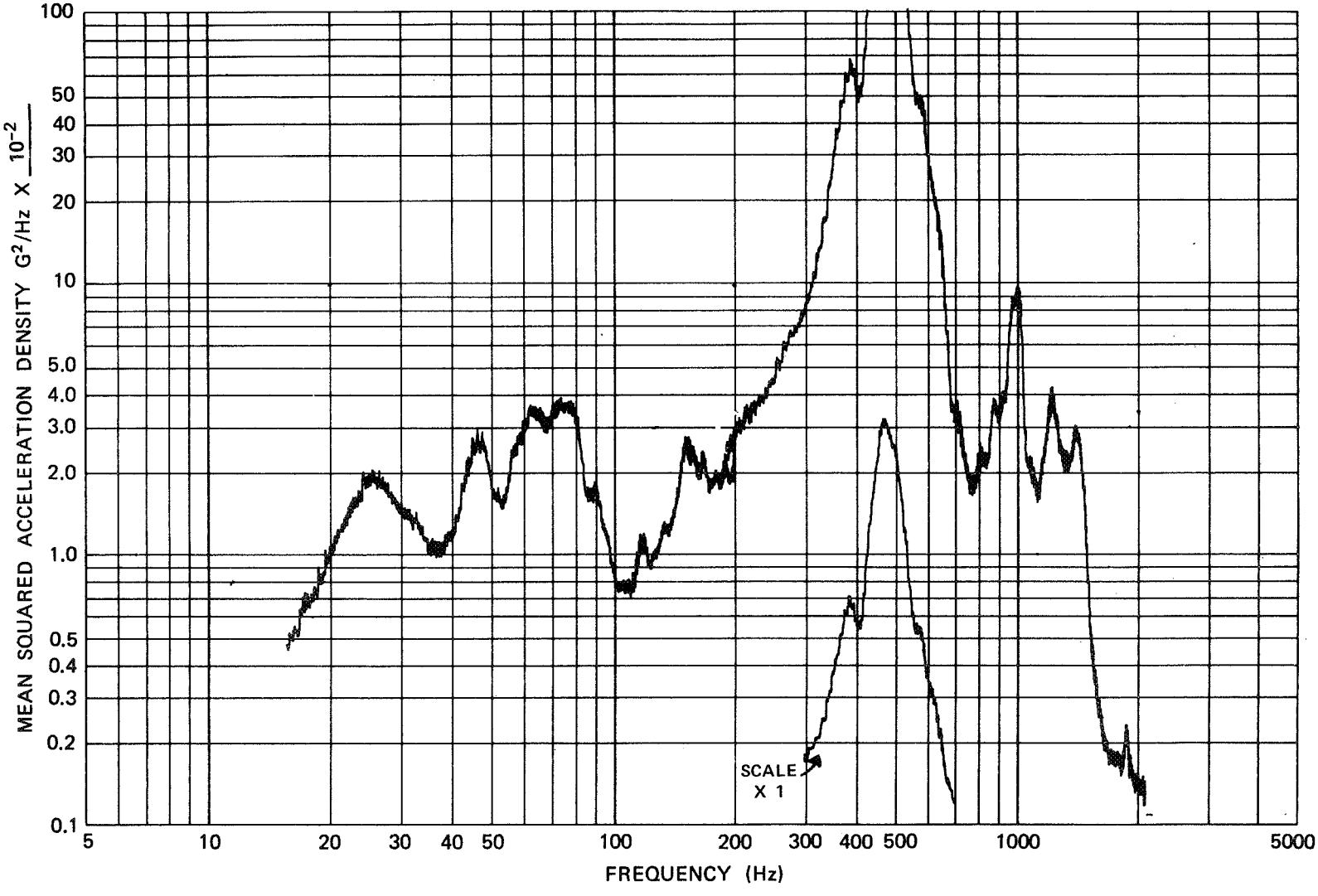

Figure 22. PSD Plot of Response at Top Shelf for Random Thrust Axis Input

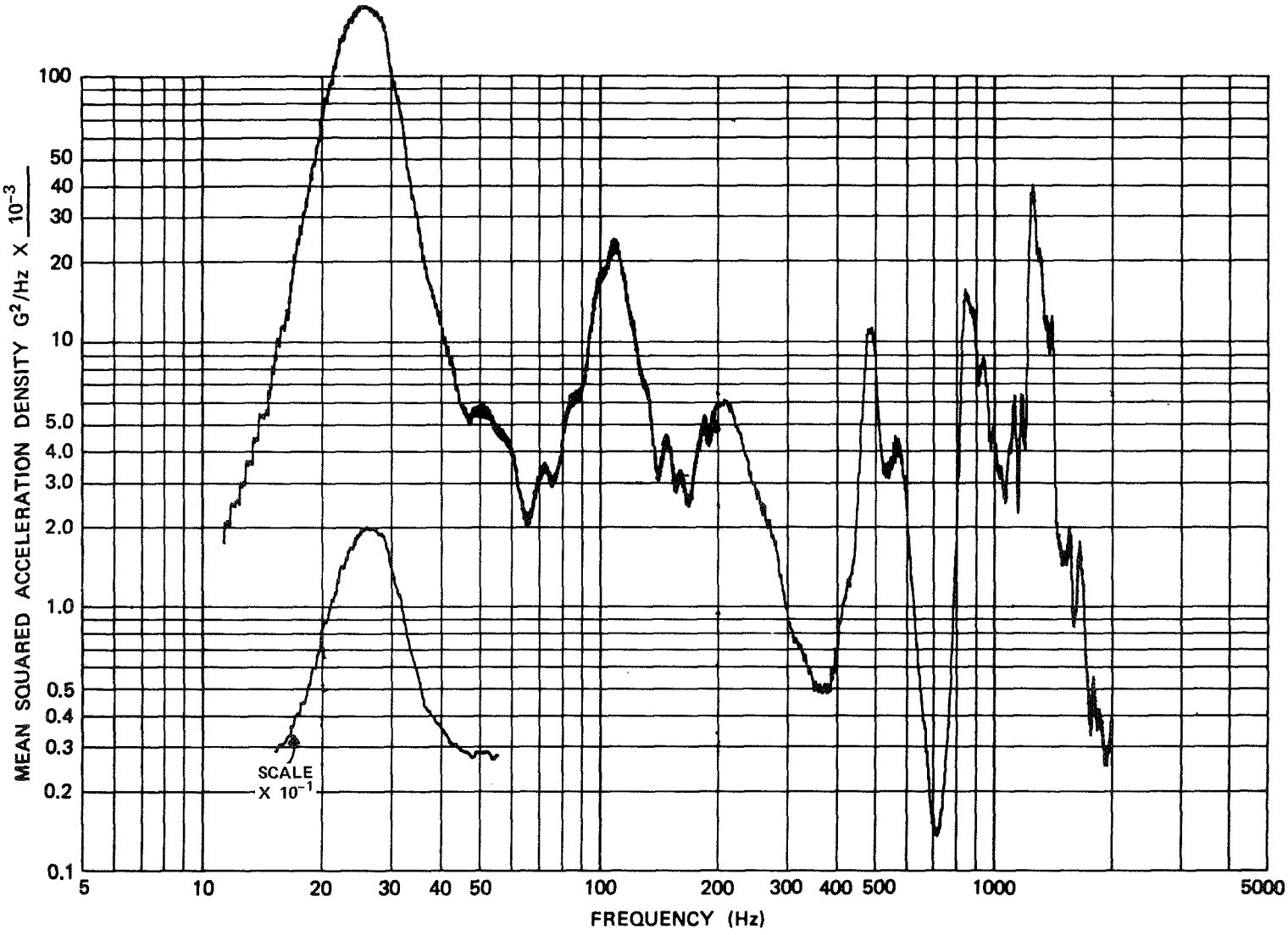

Figure 23. PSD Plot of Response at Top Shelf for Random Lateral Input

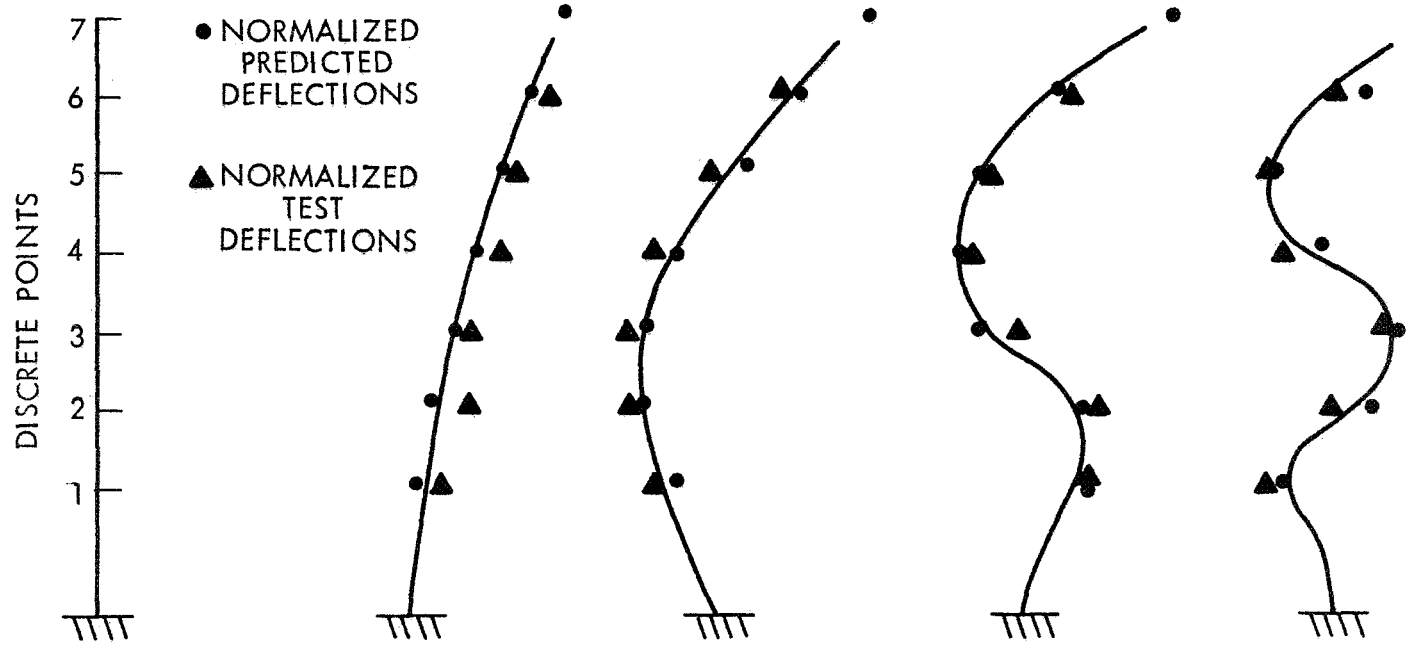

Figure 24. Mode Shapes (Theoretical and Test) of Rack with Uniformly Distributed Payload

that the loaded rack does indeed behave like the mathematical model assumed for it.

However, when a similar comparison is made for the rack/shroud configuration, deviations between the predicted and actual mode shapes are evident. This can be seen from Figure 25, which presents such a comparison for the nominal distribution. This diagram shows that the deflections at the lower shelves tend to be greater than predicted. The explanation for this lies in a shortcoming of the mathematical model. The model has a constant stiffness along its entire length, whereas this is not the case with the rack/shroud configuration. The majority of the stiffness in the system is concentrated at the top of the rack where the o-ring joins it to the shroud. This suggests that the deflection at the lower shelves should be greater than the corresponding theoretical predictions. As was stated above, this did prove to be the case. Another reason why the addition of the shroud results in deviations from the theoretical response is that this addition causes dynamic coupling to take place. The response at any point in the payload thus becomes dependent upon the natural frequencies of the longerons, the shelves, and the shroud.

CONCLUSIONS

From an examination of the results described above, it was decided that a general purpose subsystem specification could be derived which would better simulate the stresses that subsystems are subjected to when vibrated as part of a fully integrated payload.

Figure 26 presents a plot of acceleration level vs frequency. The dotted line represents the NIKE-APACHE sinusoidal vibration specification for a lateral input. Each data point represents a peak acceleration measured at one of the shelves for a particular frequency. There are four vertical groups of points which correspond to the four frequency regions at which amplifications take place. As can easily be seen, the points often indicate much higher acceleration levels than that of the input. The solid line represents the suggested specification for NIKE-APACHE subsystem sinusoidal testing (in lateral axes). Fifty percent of the data points are equal to or less than the suggested specification at the frequency in question, while the deviations of the remaining points are not nearly as great as from the present specification.

A corresponding graph for the thrust axis is shown in Figure 27. Once again, the dotted line designates the present specification, the solid line represents the peak accelerations at the various shelves. More than fifty percent of the data points are less than or equal to the suggested specification levels. As

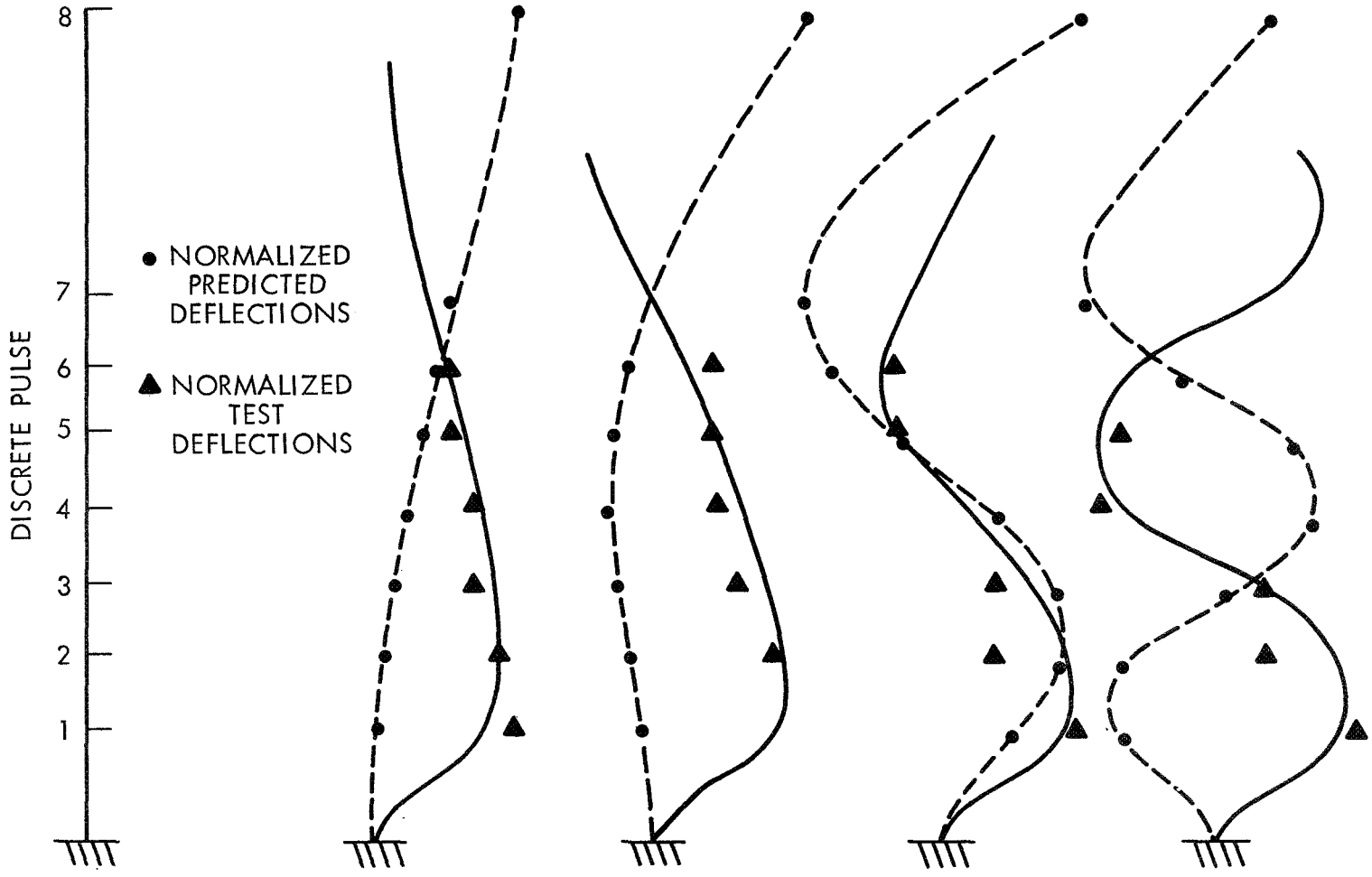

Figure 25. Mode Shapes (Theoretical and Test) of Rack/Shroud Combination with Nominal Payload Distribution

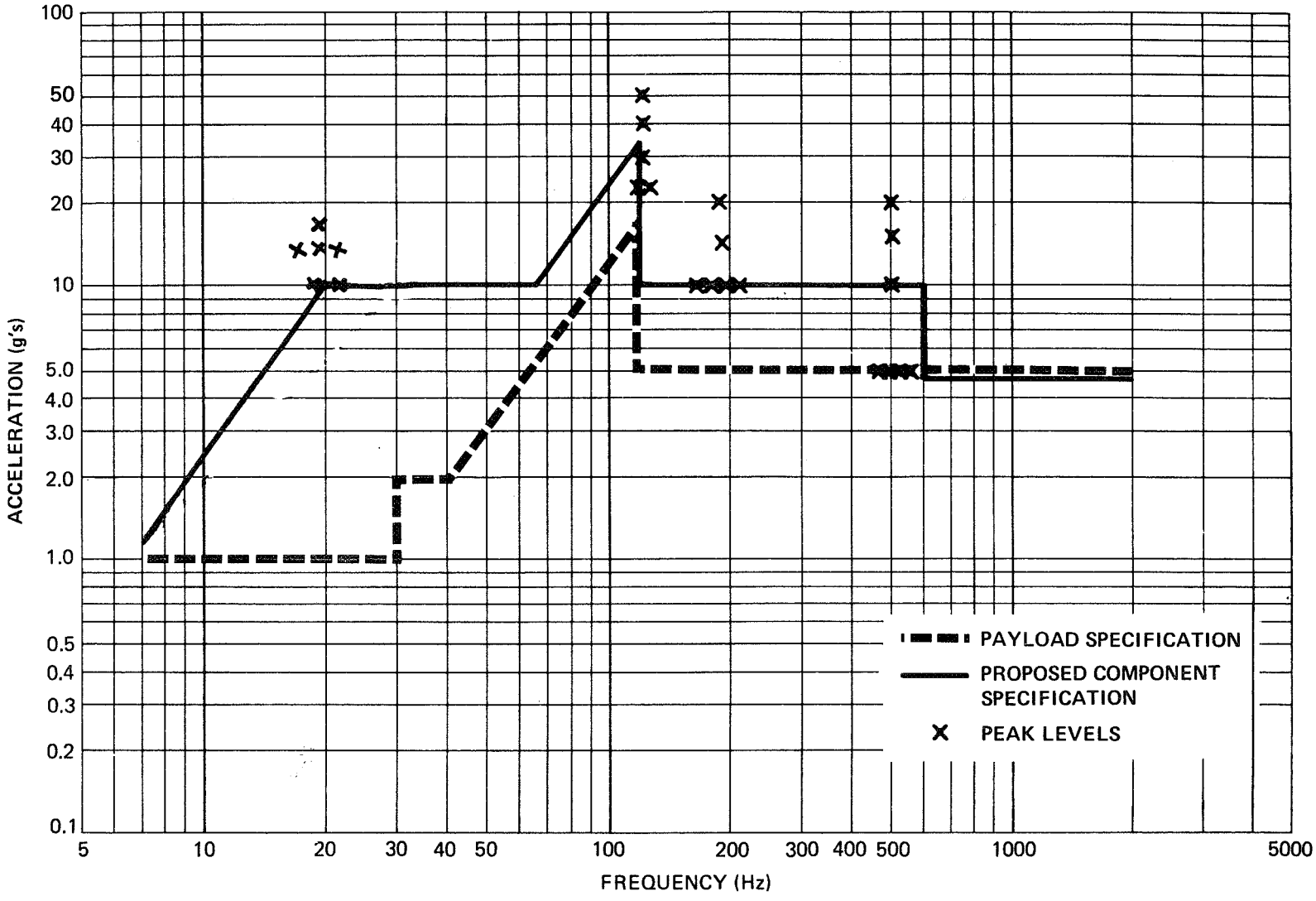

Figure 26. Proposed Lateral Sinusoidal Specification for NIKE-APACHE Components

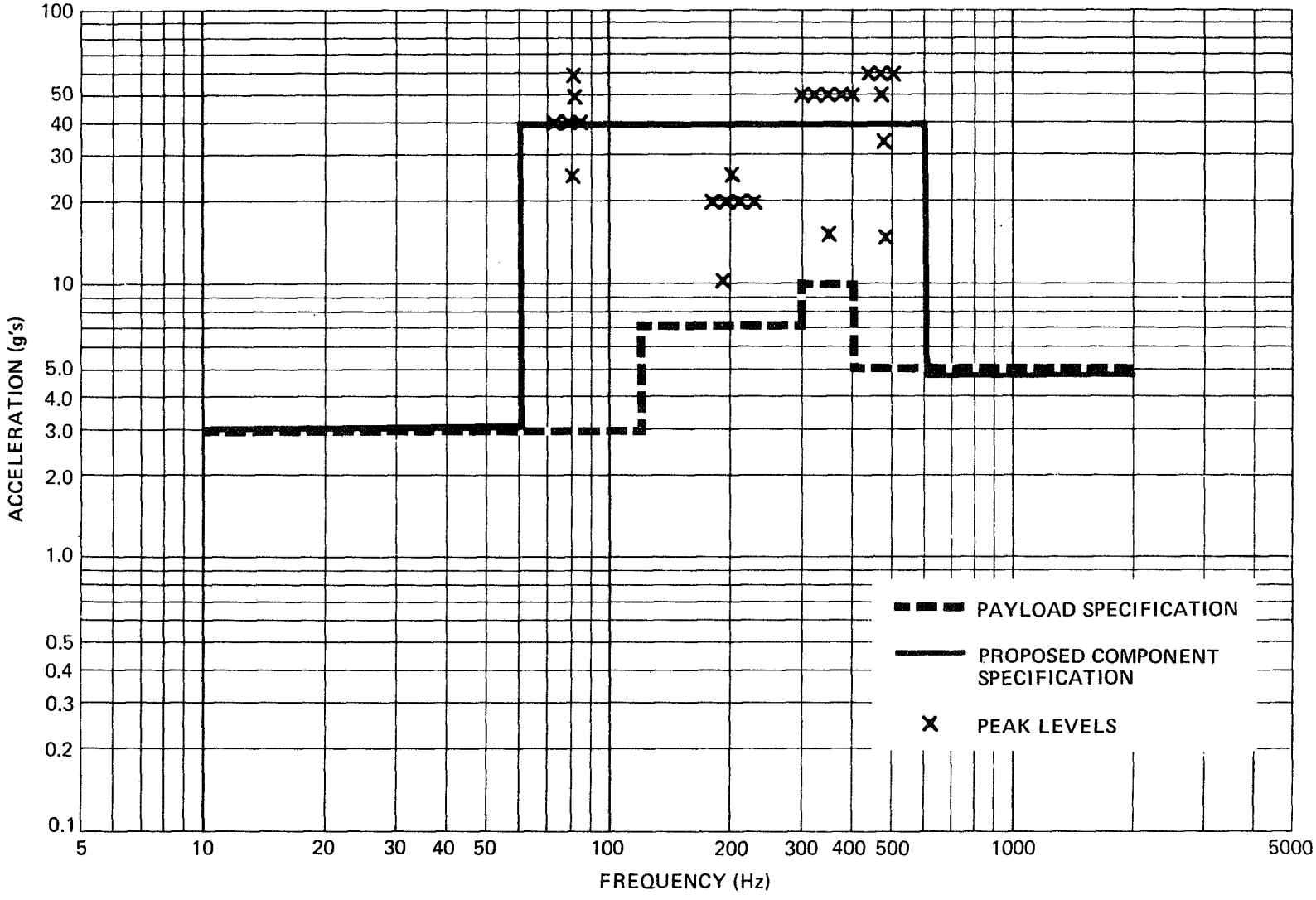

Figure 27. Proposed Thrust Sinusoidal Specification for NIKE-APACHE Components

before, the deviations of the other data points from the suggested specification are much less than from the present specification.

A brief discussion will now be presented on the methods employed in arriving at the exact levels of the proposed specification which are presented in Table 2. The knowledge obtained from the low level sweeps and the effects of the various parameters investigated were factors which were taken into consideration. For example, it was verified that the payload weight affected the frequency regions at which amplifications took place. From this information, upper and lower frequency limits, at which effects of a particular resonance would be experienced, were established. This was then taken into account in determining the different acceleration levels and the frequency range over which they acted. The proposed spec is not merely an attempt to envelope all the data points but is designed to give reasonable assurance that subsystems have been adequately tested at the subsystem level.

Table 2
Recommended NIKE-APACHE Vibration Specifications
Sinusoidal

Axis	Frequency Range (Hz)	Level (g, 0-to-peak)	Sweep Rate
Thrust z-z	10-60 60-600 600-2000	3.0 40.0 5.0	4 Octaves per minute
Lateral X-X and Y-Y	7-20 20-64 64-120 120-600 600-2000	0.5" D.A. 10.0 0.048" D.A. 10.0 5.0	4 Octaves per minute

Random

Axis	Frequency Range (Hz)	PSD Level (g^2/Hz)	Acceleration (g-rms)	Duration
Thrust z-z	20-200 200-600 600-2000	0.20 0.80 0.20	25.2	10 sec.

Table 2 (Continued)

Axis	Frequency Range (Hz)	PSD Level (g^2/Hz)	Acceleration (g-rms)	Duration
Lateral X-X and Y-Y	20-2000	0.20	20.0	10 sec. per axis

Sinusoidal Transient

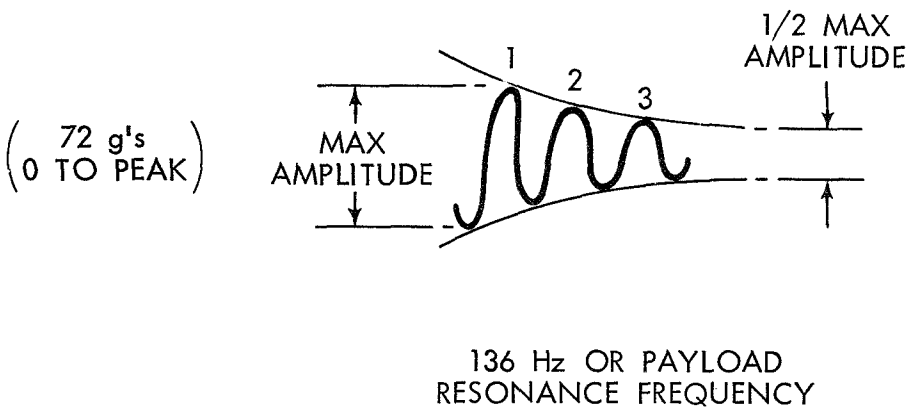

From the PSD plots obtained from the random vibration it was found that in the thrust axis the overall rms value was greater than the input rms (this was not the case in the lateral axis). Most of the energy was present in the frequency region from 200-600 Hz. For this reason it is suggested that the G^2/Hz level be increased from the payload level of 0.2 to a value of 0.8 in this region. The level would remain at 0.2 at all other frequencies. This shaped random results in an overall level of 25.2 g-rms. In the lateral axes the specification would remain the same.

The final recommendation is that the level of the decaying sinusoidal shock transient be increased. As stated before, a shock transient of 10 g's (0 to peak) consistently resulted in responses of 30 g's at all shelves for the various mass distributions. Considering this information and the non-linearity of the system in the thrust axis it is suggested that the shock transient for components be increased to a level of 72 g's (0 to peak). The present level is 36 g's.

It was felt that one sub-system spec could be recommended instead of a variable specification depending upon the location of the item in question. This

decision was based on the results of this study, which indicate that shelf location normally does not change the peak levels significantly.

It is recommended that this study be continued to determine appropriate levels for subsystems of the other types of sounding rocket payloads.